LICENCE TO McMASTER UNIVERSITY

This Thesis has been written
[Thesis, Project Report, etc.]

by Andelko Mijatovic for
[Full Name(s)]
Undergraduate course number 4K06 at McMaster University under the supervision/direction of Dr. J.H. Crocket.

In the interest of furthering teaching and research, I/we hereby grant to McMaster University:

1. The ownership of 3 copy(ies) of this work;
2. A non-exclusive licence to make copies of this work, (or any part thereof) the copyright of which is vested in me/us, for the full term of the copyright, or for so long as may be legally permitted. Such copies shall only be made in response to a written request from the Library or any University or similar institution.

I/we further acknowledge that this work (or a surrogate copy thereof) may be consulted without restriction by any interested person.

James H. Crocket
Signature of Witness, Supervisor

A. Mijatovic
Signature of Student

09/03/92
date

FLUID INCLUSIONS OF AURIFEROUS QUARTZ VEINS FROM HARRIGAN COVE, NOVA SCOTIA

Fluid Inclusions of Auriferous Quartz Veins From Harrigan Cove, Nova Scotia

April 1992

Andy Mijatovic

Title: Fluid Inclusions of Auriferous Quartz Veins From Harrigan Cove, Nova Scotia

Author: Andelko Mijatovic

Supervisor: Dr. J.H. Crocket

Date: April, 1992

In fulfilment of a Bachelor of Science Degree at McMaster University

Abstract

The Meguma Group is situated in the southeastern and southwestern regions of Nova Scotia. The Meguma Group is divided into two formations: the Goldenville and the Halifax. Both formations are comprised of A and E divisions of the Bouma sequence. Thus, the Meguma Group is a turbidite deposit.

Auriferous quartz veins strike parallel to bedding and occur between the lower Bouma cycle's E division and the overlying Bouma cycle's A division. The development of bedding-parallel veins was due to hydraulic fracturing of the Bouma units.

The bedding-parallel quartz veins were emplaced at low temperatures, from 260°C to 300°C. The fluid which precipitated the gold-arsenopyrite-quartz veins consisted of a divalent cation salt species ($MgCl_2$) and hydrosulphide ligands which were the main complexing agent of gold.

Gold was precipitated due to the reduction of sulphide ligands as they came into contact with the organic-rich slates of the E division of the Bouma sequence. Sulphide reduction was not complete, thus a large concentration of gold remained in solution later to be precipitated with arsenic in arsenopyrite

Acknowledgements

I would like to thank Dr. J.H. Crocket, my thesis supervisor, for suggesting the thesis topic and guiding me through it. I send my appreciation to David Good for his helpful commentary. And Jack Whorwood supplied his valuable time and experience on photography.

Table of Contents

Table of Figures

Table of Graphs

Tables

Chapter 1

INTRODUCTION AND BACKGROUND

Introduction (1.1)

An important type of Gold mineralization in Nova Scotia is that contained in Cambro-Ordovician slates and greywackes of the Meguma Group. The Meguma Group consists of two formations the Halifax (predominantly slate) and the Goldenville (predominantly greywacke)(see Fig. 1)(Schenk, 1970). The occurrence of gold in these formations is mainly in auriferous quartz veins which strike sub-parallel to the bedding of their host rocks (Mawer, 1986).

Approximately, one hundred and twenty vein-associated gold deposits occur over the Meguma Terrane (see Fig. 2)(Mawer, 1986). Production of gold began in the early 1860's, immediately after it was first discovered, and continued for eighty years amounting to 35,130,187 grams at grades of 8.6 to 51.4 grams per tonne (see Graph 1)(Nova Scotia Department of Mines, 1964).

Many studies have been done and papers written on the paragenesis of gold in the Meguma Zone. In this study, fluid inclusions found in the quartz veins are observed to further understand the gold mineralization and the origin of the veins. The major objective, in this paper, is to define the properties of the fluids which precipitated the gold.

Geological Map of the Meguma Terrane

Nova Scotia

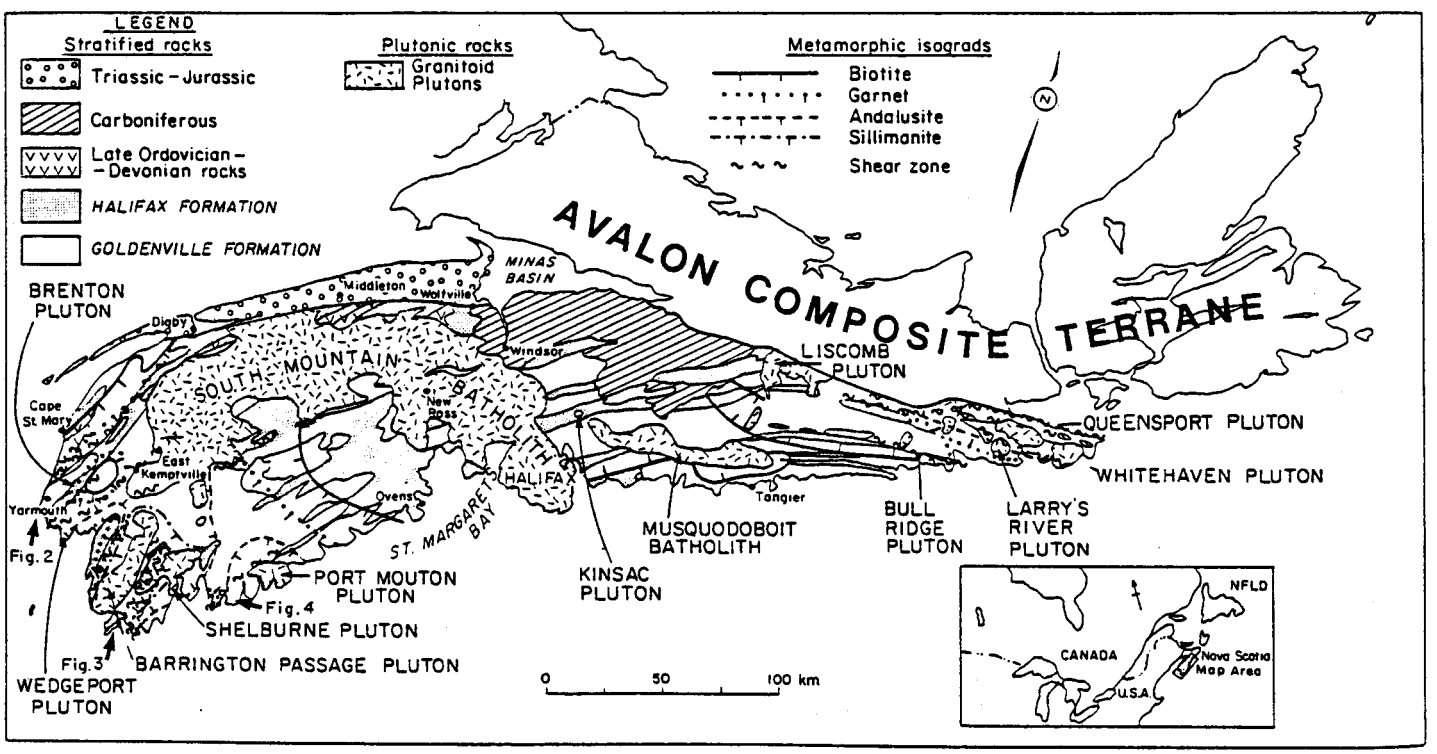

Figure 1 (Dallmeyer and Keppie, 1987)

Meguma Terrane of Nova Scotia,

Showing Bedding-Concordant Gold-Quartz Vein Deposits

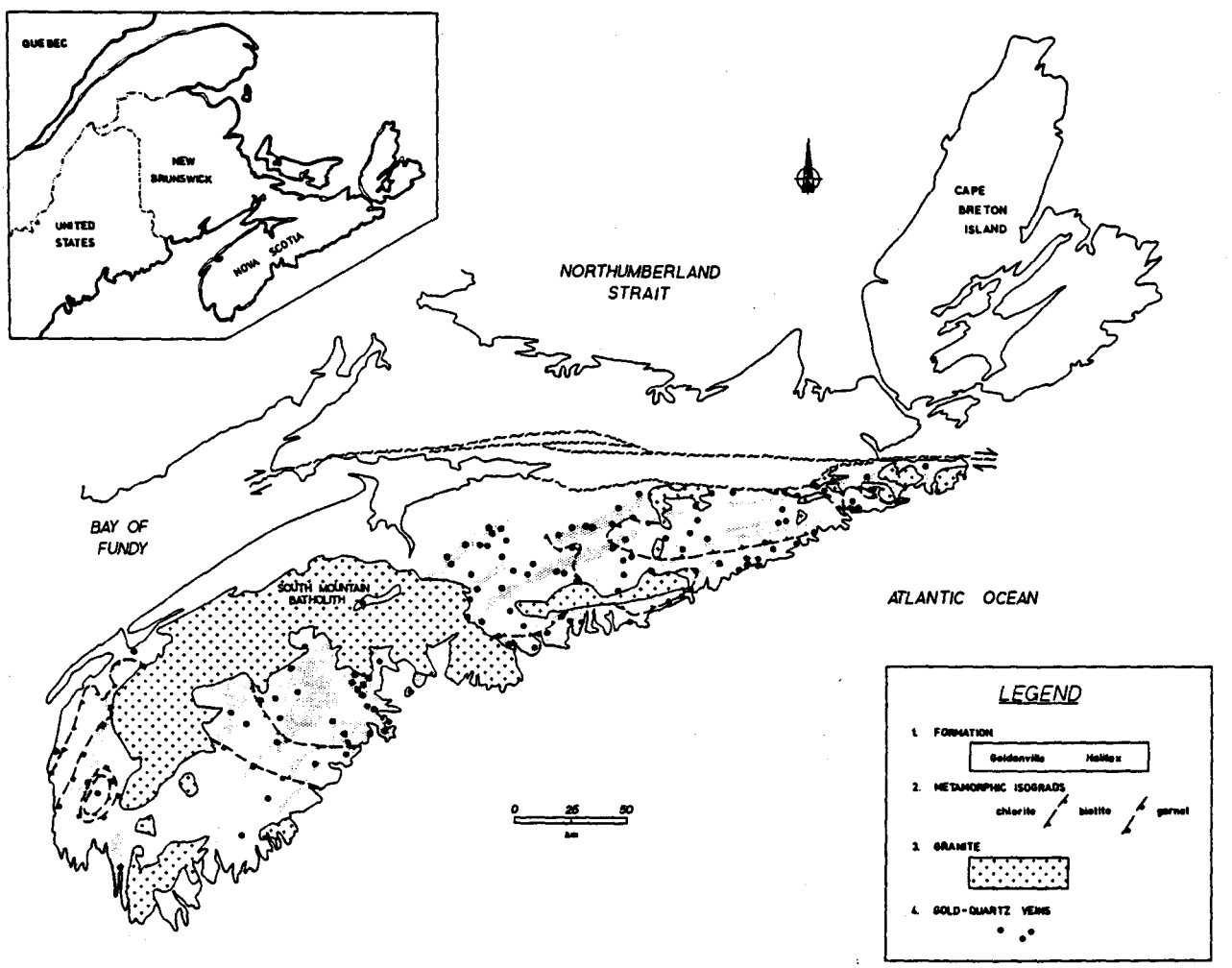

Figure 2 (Mawer, 1986)

Gold Production From Meguma Rocks, Nova Scotia Over 100 Years, Expressed as Percent of Total Reported Production

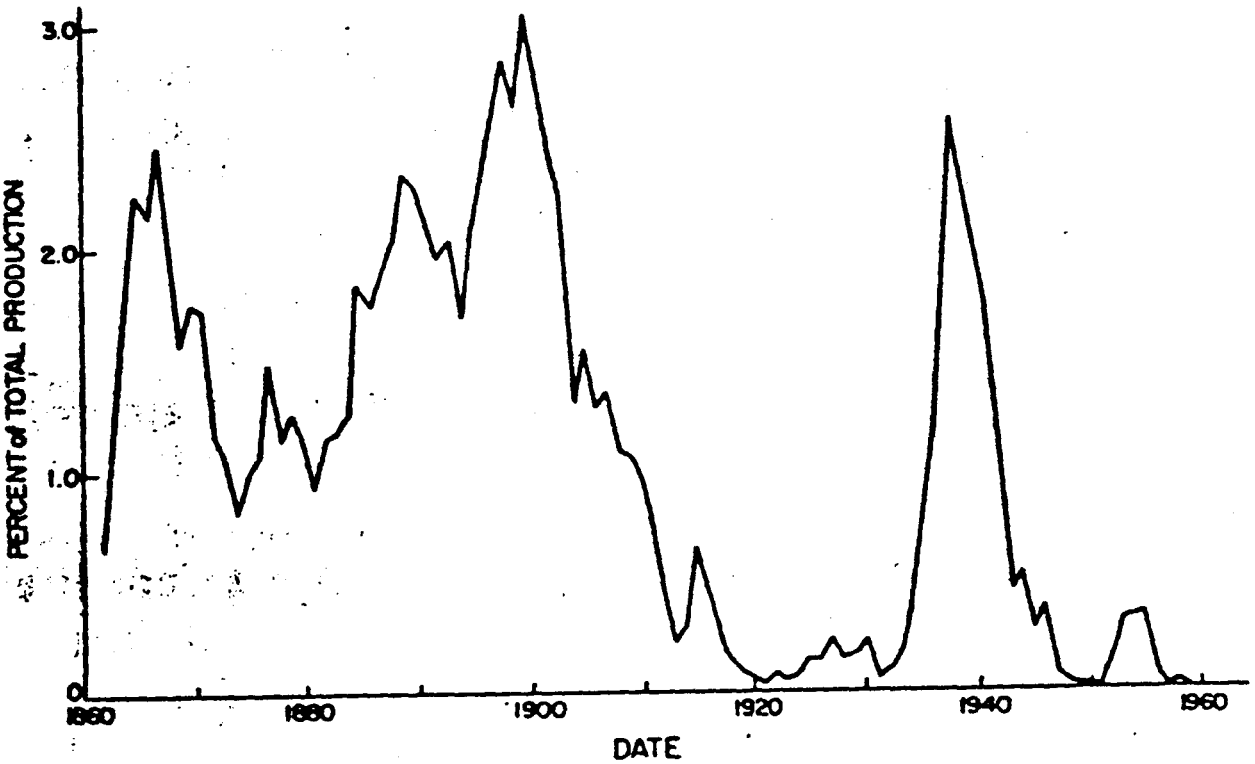

Note: The peaks and valleys tend to reflect the business cycles and technological advancements for the period.

Graph 1 (Graves and Zentilli, 1982)

Geology and Location of Study Site (1.2)

The Meguma Group lies in the southeastern and southwestern parts of the Nova Scotia mainland. The group is intruded by the South Mountain Batholith of Nova Scotia (see Fig. 1)(Taylor and Schiller, 1966).

The thickness of the group is speculative since the base is nowhere exposed, but an estimate of at least 6096m thick is probable and in some localities a thickness of 9144m is suggested (Taylor and Schiller, 1966).

Geologically, the Meguma Zone can be considered pre-Acadian domain, separated from the Avalon Zone by the east-striking Glooscap Fault (see Fig. 3)(Schenk, 1978; King and MacLean, 1970; Eisbacker, 1969). These two domains form the basement of a post-orogenic Glooscap domain (Graves and Zentilli, 1982).

The Meguma Group is considered to be turbiditic in origin (see Fig. 4 and 5)(Schenk, 1981). Turbidites are deposited from a turbidity current; nearly complete Bouma cycles are typically developed and show the classic features of deposition from turbidity currents including graded bedding, moderate sorting and well developed primary structures in the sedimentary sequence (Boyle, 1986). Meguma rocks contain relatively few fossils (Schenk, 1981).

Surface Projection of Minas Geofracture

Including the Glooscap Fault

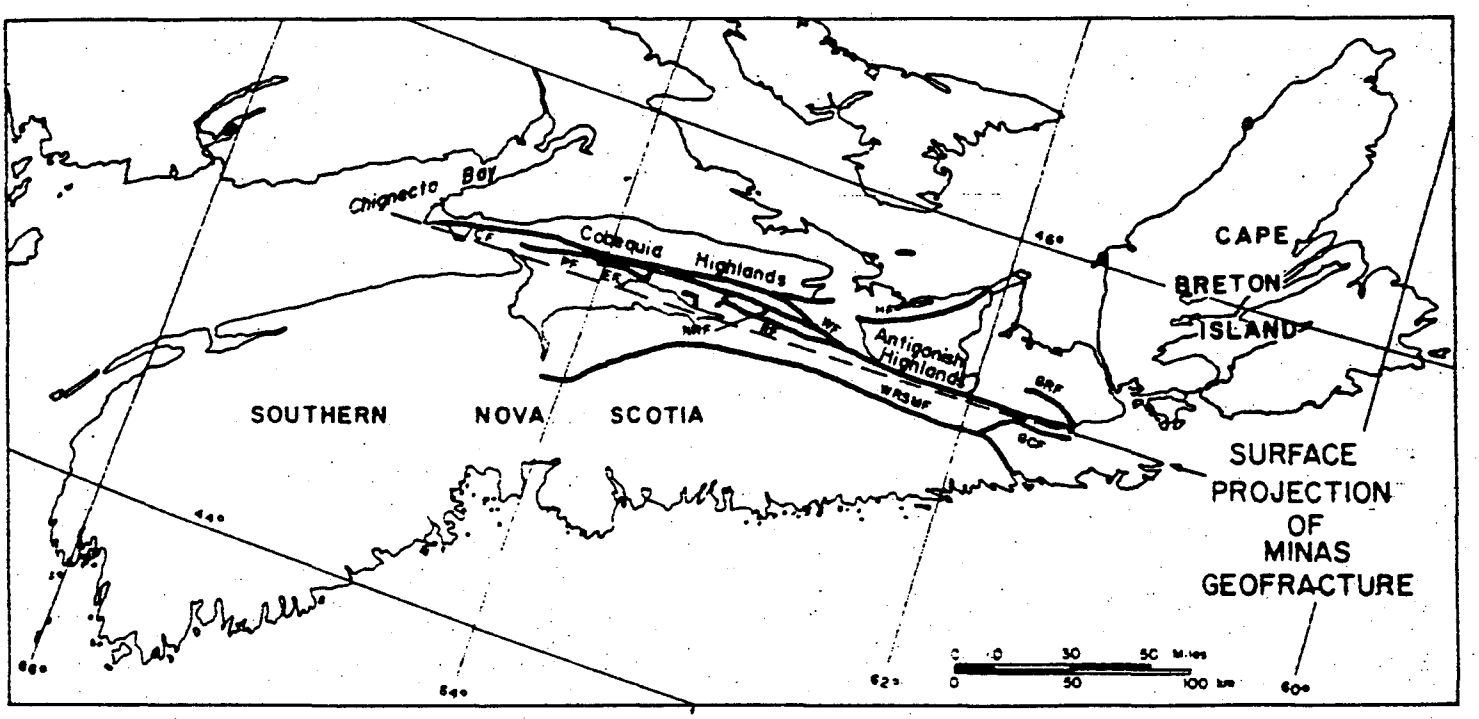

Figure 3 (Keppie, 1982)

Geology of the Central South Pit Locality

Showing 12 Bouma Units

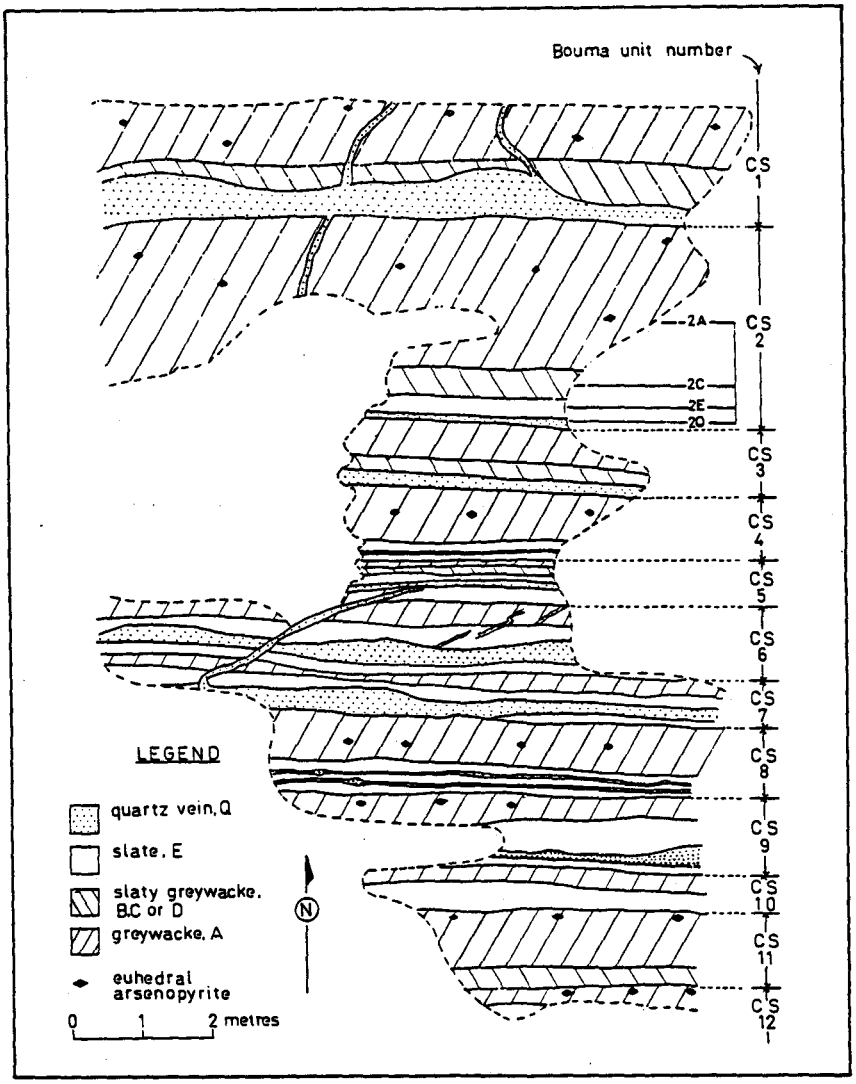

Note: Beds face south with an average dip of 070° south. Bedding-parallel and discordant quartz-veins are shown.

Figure 4 (Crocket et al., 1986)

Typical Bouma Sequence

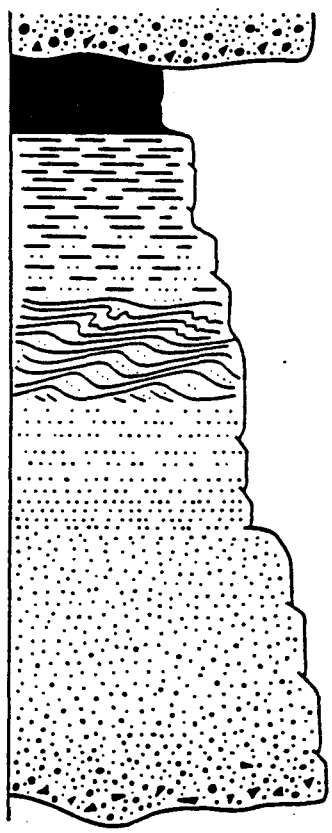

Note: A and E(t) beds are present at the Central South site.

Figure 5 (Walker, 1984)

The Meguma Group's two formations are examples of the lithological A and E(t) units of the Bouma cycle.The Goldenville Formation consists predominantly of thin- to thick-bedded, lithic greywacke and feldspathic quartzite. The Halifax Formation is chiefly thinly bedded slate, siltstone and argillite (Taylor and Schiller, 1966).

The Meguma Group is both regionally and contact metamorphosed; recrystallization was the result of both types of metamorphism which generally reached greenschist grade (Taylor and Schiller, 1966).

Structurally, these rocks are deformed by major, upright, east-northeast trending, subhorizontal folds cut by weakly developed cross folds (Fyson, 1966).

This study reports on the rocks of the Harrigan Cove gold district which is located approximately 100 km east of Halifax. Some 0.5km north of the Harrigan Cove post-office off Hwy 7, trenching and stripping have exposed auriferous quartz veins, samples of which were taken for this study (see Fig. 6). The greywacke and slate bedrock, in this area, is in the Goldenville Formation (Crocket et al., 1986).

The Harrigan Cove gold district has been studied by Anderle (1974), Kretschmar(1983), Henderson(1983b) and Crocket et al.(1986). The following description is summarized from the latter group of authors. As shown in Figure 4, the host rocks are predominantly greywacke and slate, comprising the A and E divisions, respectively, of the Bouma sequence.

Site Location of Thesis Harrigan Cove, Nova Scotia

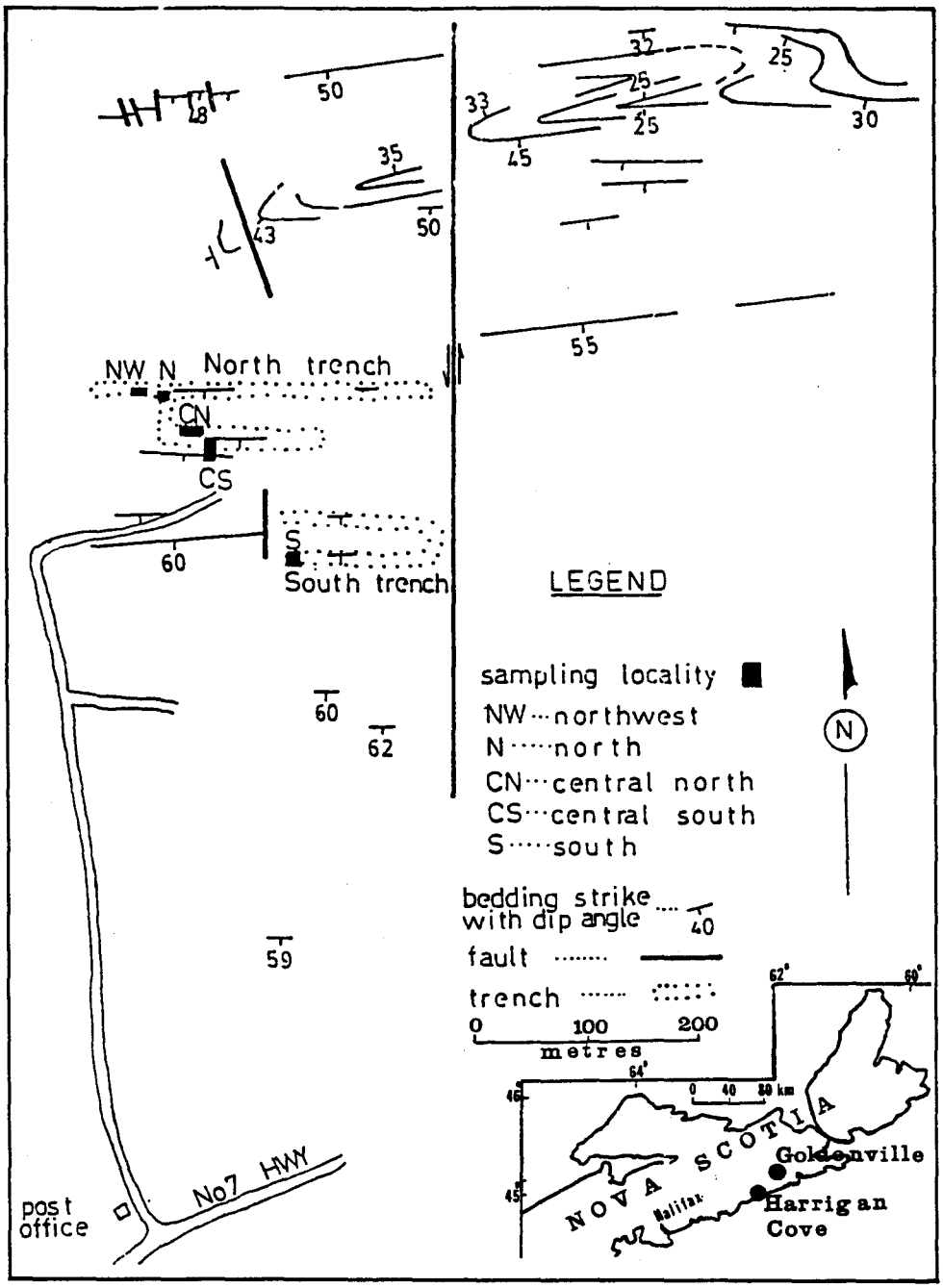

Figure 6 (Crocket et al., 1986)

Occasionally, C division layers of slaty greywacke are included at the stratigraphic top of the A division greywackes. Local bedding dips from 60° to 85° south and strikes approximately 090°. The majority of quartz veins are parallel to bedding and are hosted either within E division slates or at the contacts of E divisions and the base of the overlying A division greywacke beds of the overlying sequence. Thinner, discordant quartz veins also occur, these appear to originate from thicker concordant veins.

Geological History (1.3)

The Appalachian Orogen of North America is divisible into five tectonolithologic zones which range in age from the late Pre-Cambrian through the early Palaeozoic (see Fig. 7 from Schenk, 1981). Four of these zones can be traced from the southern Appalachians to Newfoundland (Williams, 1978b). These zones are the eastern continental margin of North America, the now discontinuous remnants of an early Palaeozoic ocean floor, the western continental margin of the Avalon micro-continent with offshore welts, and the Avalon micro-continent itself. The Meguma Zone is the fifth domain and it is an exception, because it cannot be traced either to the southwest or the northeast (see Fig. 8). Schenk (1970) proposes the source area lay to the southeast of the zones present location.

Tectonolithologic Zones of the Appalachian Origin,

and Their Possible Origins

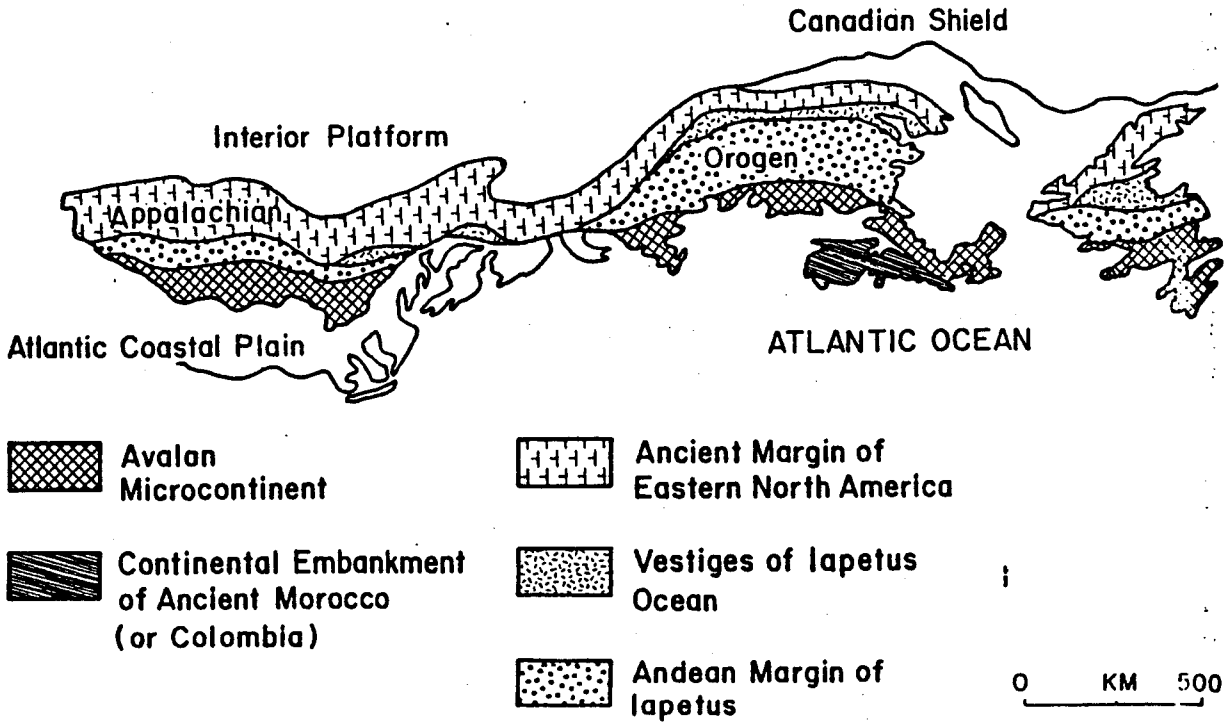

Figure 7 (Williams, 1978b)

Meguma Zone as a Suspect Terrane

Figure 8 (Schenk, 1981)

The strata of the Meguma Group is conformable, recording a continuous process of sedimentation from Cambrian to early Devonian - an interval of 200 million years (Schenk, 1970).

The two formations of the group closely resemble modern overbank turbidites and contourites of the Laurentian Fan (Stow, 1979). The Meguma Group, as Schenk (1981) interprets, is a deep-sea fan complex that grades upward through slope and outershelf paleoenvironments. The source area for the Meguma Group was a low lying, deeply eroded, granodioritic Pre-Cambrian shield characterized by a long-term passive margin possibly with a wide continental shelf.

According to Keppie (1982), the Meguma Zone came to its present location by dextral transcurrent motion along the Minas Geofracture, which became active in Early Devonian during the Acadian Orogeny (see Fig. 9).

Approximately, 385 to 410 million years ago the Meguma Zone underwent regional folding with associated cleavage formation under greenschist facies metamorphic conditions (Dallmeyer and Keppie, 1987). A second low pressure metamorphic event occurred during the emplacement of granitic plutons around 360 and 373 million years ago (see Table 1).

Middle Devonian Palinspastic Map of Nova Scotia

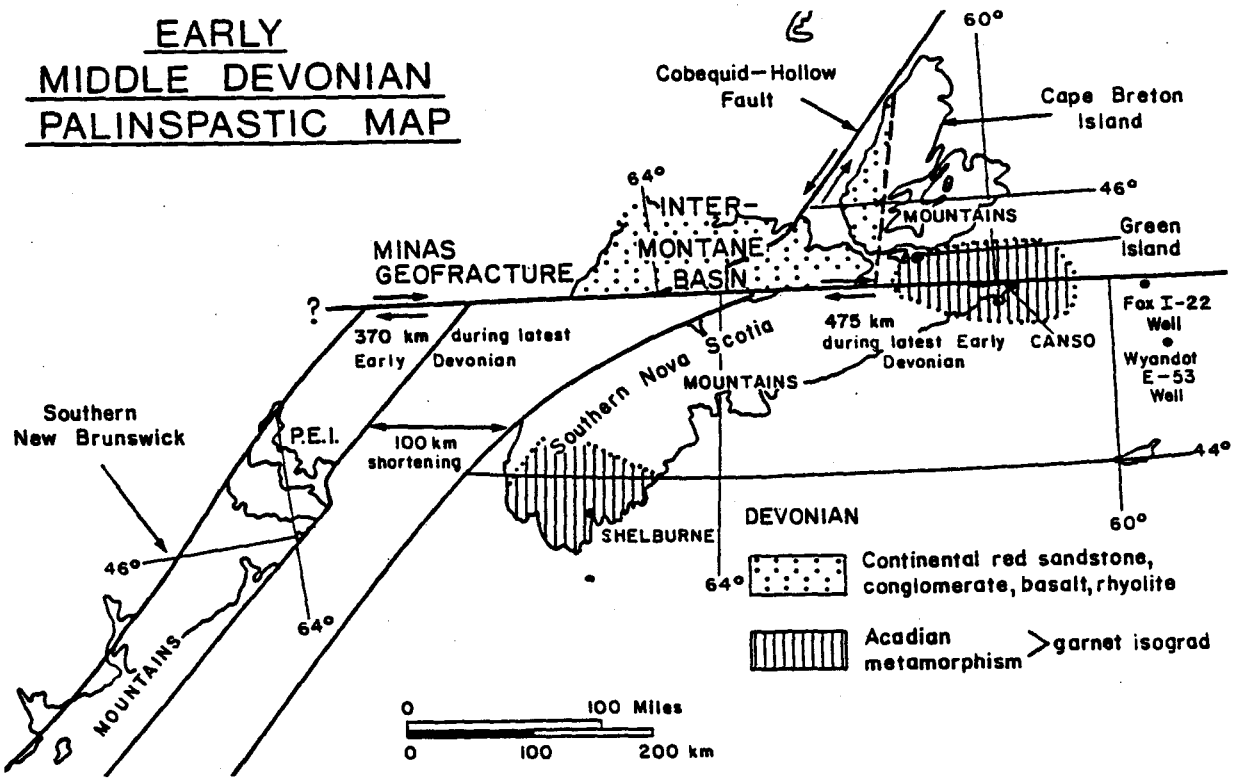

Figure 9 (Keppie, 1982)

Table 1

Geological Events Occurring in Chronological Order on the Meguma Terrane

Event	Age (Ma)	Reference
(1) Carboniferous and post-Carboniferous		
(I) Mafic igneous activity	202	Poole *et al.* (1970)
(II) Minas Geofracture	Dev.–Carb.–Perm.	Keppie (1982)
(III) Maritime disturbance	Late Carboniferous	Poole (1967)
(IV) Dunbrack Pb–Zn–Ag deposit	304	MacMichael (1975)
(V) Southern satellite plutons	350–258	Reynolds *et al.* (1981, 1984)
(2) Granite intrusion age	372–361	Clarke and Halliday (1980)
(3) Thermal aureole reset age	400–370	Reynolds *et al.* (1973)
(4) Acadian deformational age	415–400	Reynolds and Muecke (1978)
(5) Meguma Group depositional age	Cambro-Ordovician	Schenk (1983)
(6) Meguma Group detrital mica age	496–476	Poole (1971)

Gold Mineralization and History (1.4)

The occurrence of gold in the Goldenville Formation of the Meguma Group is in quartz veins (Henderson and Henderson, 1986). These veins are divided into three categories (see Fig. 10): (1) subparallel to bedding, (2) en echelon arrays within slate interbedded with thicker arenaceous metawacke, and (3) perpendicular to fold hinges within some metawacke beds. Categories (1) and (2), Henderson and Henderson report, contain gold. The majority of veins hosting gold are confined to regions below the biotite grade of regional metamorphism (Newhouse, 1936).

The gold-hosting veins consist of coarse quartz, with some carbonate, chlorite and white mica. Arsenopyrite porphyroblasts are scattered throughout the country rock and may constitute up to 10% of the auriferous quartz veins (Henderson and Henderson, 1986). Brooks et al. (1982) noted earlier that the arsenopyrite has an intimate relationship with gold. They had compared the abundance of gold in arsenopyrite with pyrite, quartz and country rock and found averages of 4311 ppb, 76 ppb, 1.9 ppb and 1.0 ppb, respectively. This relationship had lead Boyle (1979) to suggest that arsenopyrite and gold share a solid solution relationship.

Faribault (1899) classified the bedding parallel veins in the Goldenville Formation as anticlinal saddle reefs a terminology later accepted by Keppie (1976). In Ramsay (1974), it was shown that saddle reefs form late in strain history of chevron folds, and are restricted to dilatant openings in fold hinge regions.

Henderson and Henderson (1986) argue against this notion, and show that the auriferous bedding-parallel veins are not restricted to fold hinge regions and that they predate the folding.

Graves and Zentilli (1982) proposed a model for the development of bedding-parallel veins in which the veins are a result of hydraulic fracturing under orogenic stress during greenschist grade metamorphism (see Fig. 11). Their model depends on the assumption that fluids released by dehydration reactions could not escape so that pore fluid pressures eventually exceeded the local tectonic stress. Henderson (1983a) argues that the distribution of white mica inclusions in quartz crystals within the bedding-parallel veins is due to crack-seal mechanisms of rock deformation (Ramsay, 1974) a suggestion that supports Graves and Zentilli (1982).

Faribault's "pay zone hypothesis" (1899) states, that besides the formation of ore zone in bedding-parallel veins or saddle reefs, anticlinal domes are ore zones as well. His work also reveals that many interbedded veins are richer both near the intersections with angular or branching veins and in rolls or minor folds.

Types of Quartz Veins which occur

in the Meguma Group

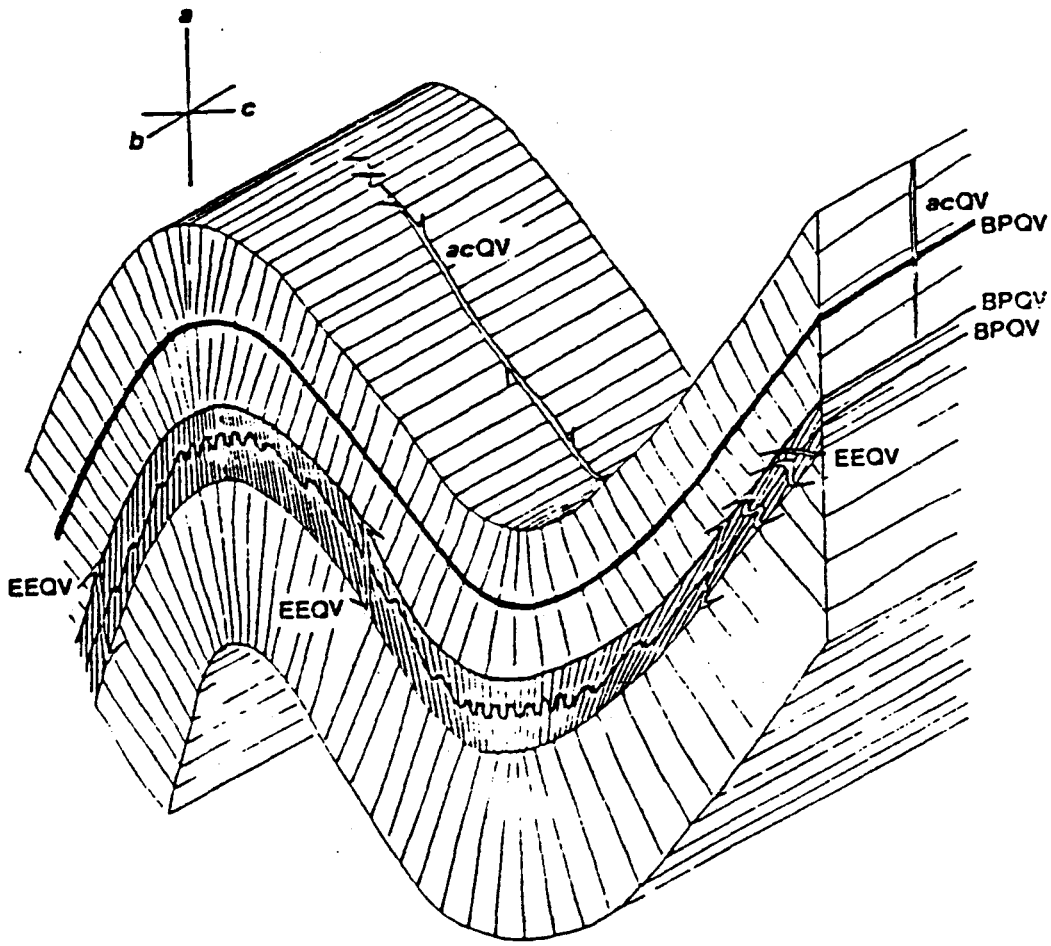

Legend

acQV..perpendicular to hinge vein

EEQV..en echelon vein

BPQV..bedding-parallel vein

Figure 10 (Henderson and Henderson, 1986)

Bedding-Parallel Quartz Vein

Produced by Hydraulic Fracturing

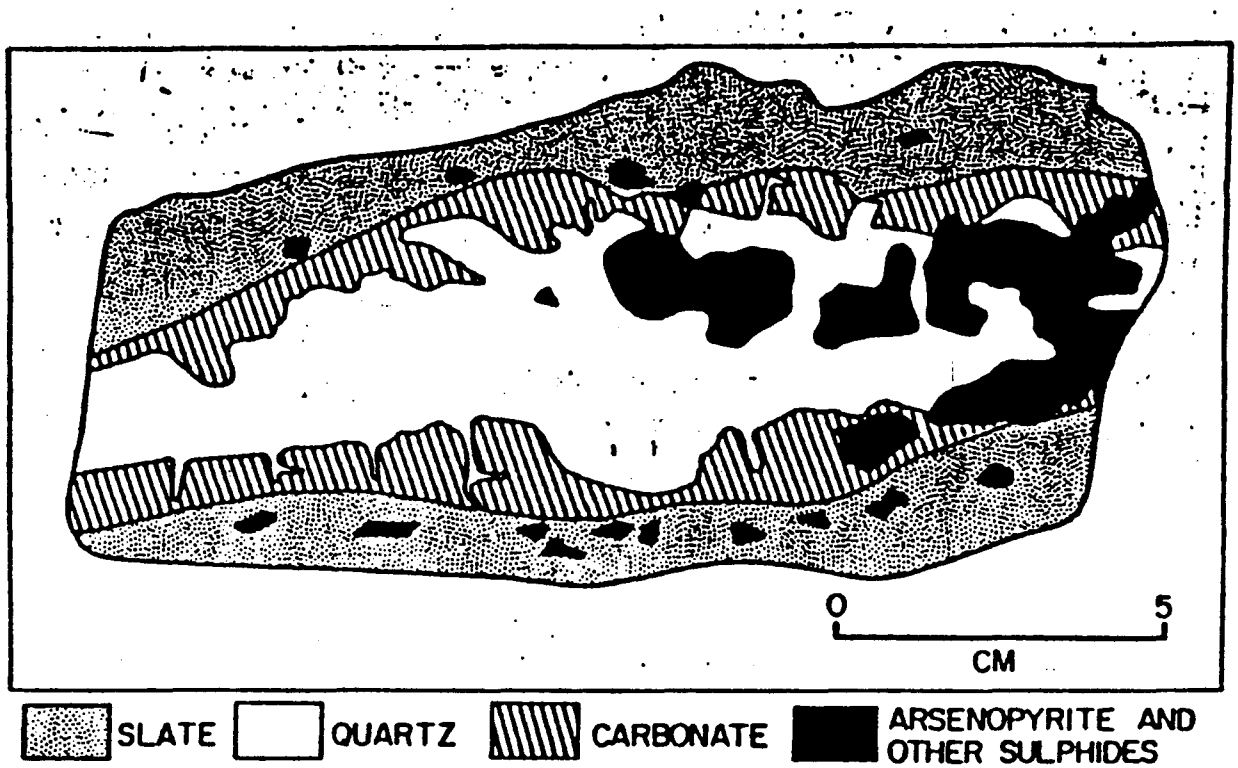

Figure 11 (Graves and Zentilli, 1982)

Fluid Inclusion Studies (1.5)

From the Dictionary of Geological Terms (3rd edition, 1984, Bates and Jackson) a fluid inclusion is defined as " a tiny cavity in a mineral, 1.0 - 100.0 microns in diameter, containing liquid and/or gas, formed by the entrapment in crystal irregularities of fluid, commonly that from which the rock crystallized" (see Fig. 12).

The first specific description of inclusions was by Abu Reykhan al-Biruni from the eleventh-century (Lemmlein, 1950). Robert Boyle's description of a large moving bubble in quartz (Boyle, 1672) is the first reference in English. But, it was Sorby's (1858) investigations that hypothesized the gas bubbles present in the fluid of most inclusions are the result of differential shrinkage of the liquid and the enclosing mineral during cooling from the higher trapping temperature to the temperature of observation that showed the geological potential of fluid inclusion studies.

In spite of limitations, H.C. Sorby's work has stood the test of time; many of his observations are still valid and useful in today's technological world.

Fluid inclusions may represent actual samples of fluids existing at the time the rock was formed, regardless of their origin and history. Thus, inclusions provide important clues in understanding the temperature, pressure, density and composition of the fluids that formed or traversed the rock (Roedder, 1984).

Two Phase Fluid Inclusion

in Quartz Crystal

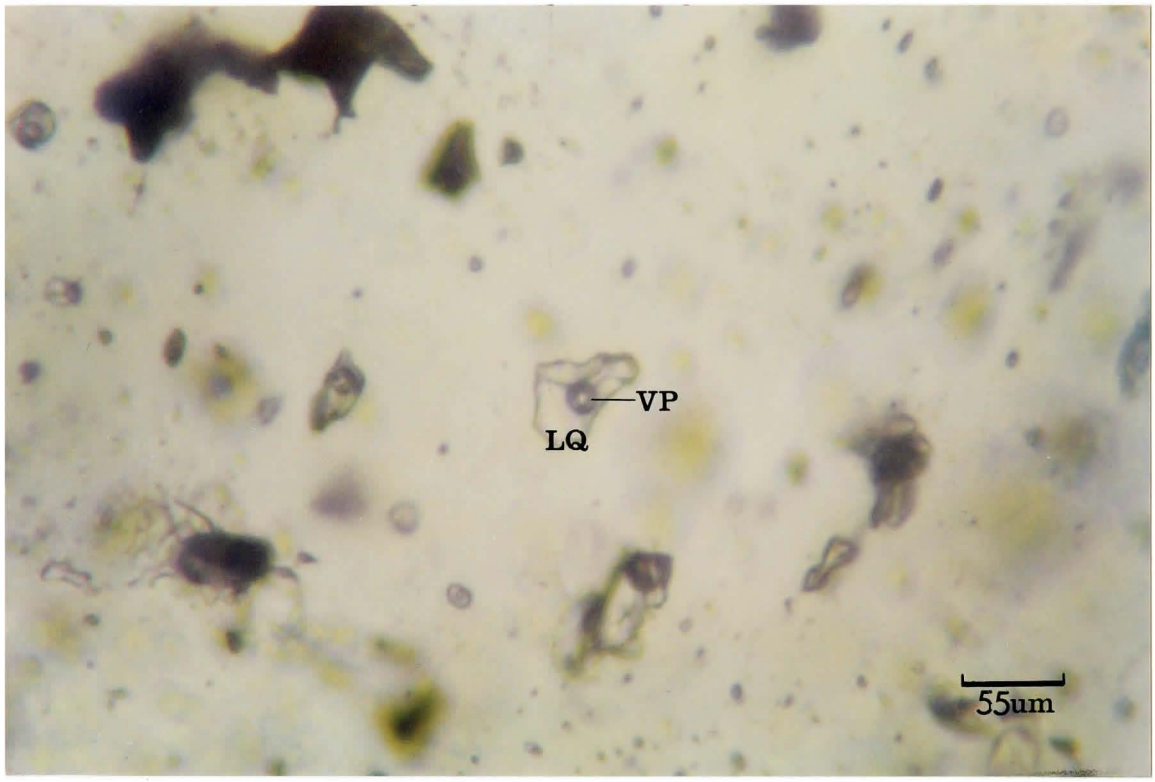

Legend

LQ...liquid phase

VP...vapour phase

Figure 12

Inclusions formed during the primary growth of a mineral (primary or P-inclusion) are distinguished from inclusions which formed in a later process after the crystal has been formed (secondary or S-inclusion)(see Fig. 13). The generally accepted mechanism for forming secondary inclusions involves the development of post-crystallization fractures initiated during mechanical or thermal stress. These cracks are later sealed by fluids that form the characteristic trails (Shepherd et al., 1986). Some authors (eg. Roedder, 1984) distinguish a third genetic class, intermediate between P- and S-inclusions which are termed pseudo-secondary or PS-inclusions (see Fig. 13). PS-inclusions are assumed to develop in a similar way to S-inclusions, the only difference is that fracturing and healing take place before crystal growth is terminated. Thus, P- and PS-inclusions reflect the character of the fluids present during growth, whereas S-inclusions represent later fluids possibly unrelated to those responsible for primary growth.

Previous work on the fluid inclusions found in the quartz veins of the Meguma Group was done by Graves (1976) as a M.Sc. thesis at Dalhousie University, Halifax, Nova Scotia. Graves' work was an addition to his thesis and encompassed a greater research area. This paper deals specifically with the quartz veins found in the Central South trench of the Harrigan Cove gold district.

Types of Fluid Inclusions

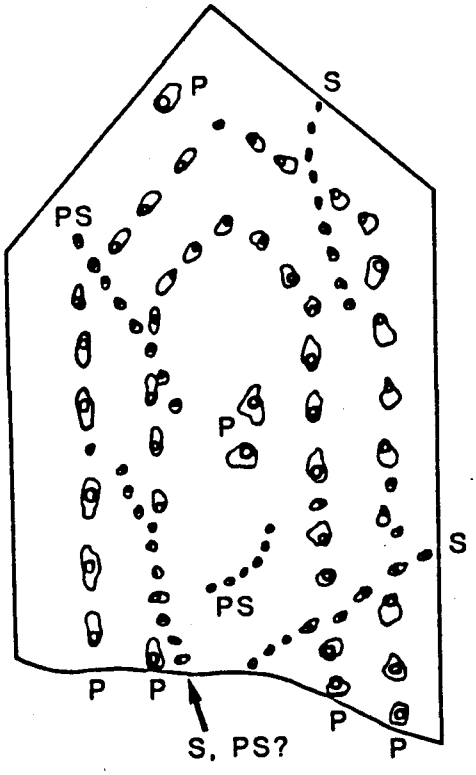

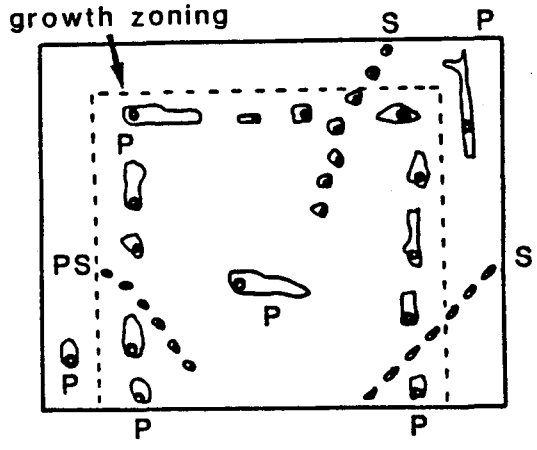

Legend

P..primary inclusion

PS..pseudo-secondary inclusion

S..secondary inclusion

Figure 13 (Shepherd et al., 1985)

Chapter 2

ANALYTICAL METHODS

Inclusion Slide Description (2.1)

Before any inclusion work commenced, the first step taken was the petrographic description of inclusion slides. Such a description included determining mineralogy, lithology and taking photographs of characteristic properties.

Optical examination of the thin-sections was conducted using a transmission and reflective light microscope. The information obtained using simple optical techniques allowed the researcher to extend the descriptions made on the mineralogy and lithology of the samples. The sections were doubly polished (top and bottom) slices of approximately 150 microns thickness prepared by Vancouver Petrographics Ltd of Langley, B.C..

Preparation of Inclusion Slides (2.2)

Firstly, the inclusion slides were cut with a bandsaw, into four sections to allow the quadrants to fit properly into the optical window of the heating/freezing stage which was approximately 1cm in diameter. After the slides were cut, they were immersed in acetone, for a period of 24 hrs, to dissolve the resin which held the inclusion slide to the glass slide.

In the second step, two quadrants from each slide were used for heating observations and the remaining two quadrants were used for freezing studies.

The heating procedure used an electric torch to heat a current of air which flowed across the sample in the heating/freezing chamber. The air rate was 30 standard cubic feet per hour (scfh). The specimen temperature was measured by a thermocouple in contact with the sample. The temperature of the inclusion was increased until homogenization occurred. Also, the reappearance temperature of the bubble was recorded as well.

During the freezing procedure, liquid nitrogen vapour was used to cool the inclusions below the first-melt temperature, the temperature of which the entire inclusion was frozen. Then the inclusion was allowed to warm-up in a nitrogen gas flow of 20 scfh and with the aid of the thermocouple, the first-melt temperature and the last-melt temperatures were recorded.

Before either heating or freezing of the inclusions was done, a complete description of the studied inclusion was noted. Such observations included classifying the inclusion (ie: primary, pseudo-secondary or secondary), size, shape and volume of fill. The volume of fill is defined as

$$F = V_L/(V_L + V_V) \qquad \text{eq. 1}$$

where V_L is the volume of liquid phase present

V_V is the volume of vapour phase present

From these data a preliminary classification of the inclusion as primary, pseudo-secondary or secondary was made.

Analysis (2.3)

After all the data was collected a complete analysis of the work was done. Part of the analysis was to use various types of graphs, including histograms and phase diagrams, to define the density and composition of the inclusions.

Equipment Used (2.4)

Figure 14 illustrates the apparatus used in this study.

Legend

(1)...JVC Camera modal no. GX-S700U

(2)...JVC Monitor

(3)...Nikon Biological Microscope Optiphot

(4)...Trendicator Temperature Gauge

(5)...Trendicator Air/Nitrogen Gauge

(6)...Thermocouple

(7)...Heating/Freezing Stage

(8)...Sample Position in Glass Window

(9)...Electrical Heating Conductor Wire

(10)..Liquid Nitrogen Vapour Tubing

(11)..Liquid Nitrogen Dewar Flask

(12)..Compressed Air/Nitrogen Flow Tubing

(13)..Air/Nitrogen Gauges

(14)..Compressed Air/Nitrogen Tanks

(15)..Thermocouple Electrical Cord

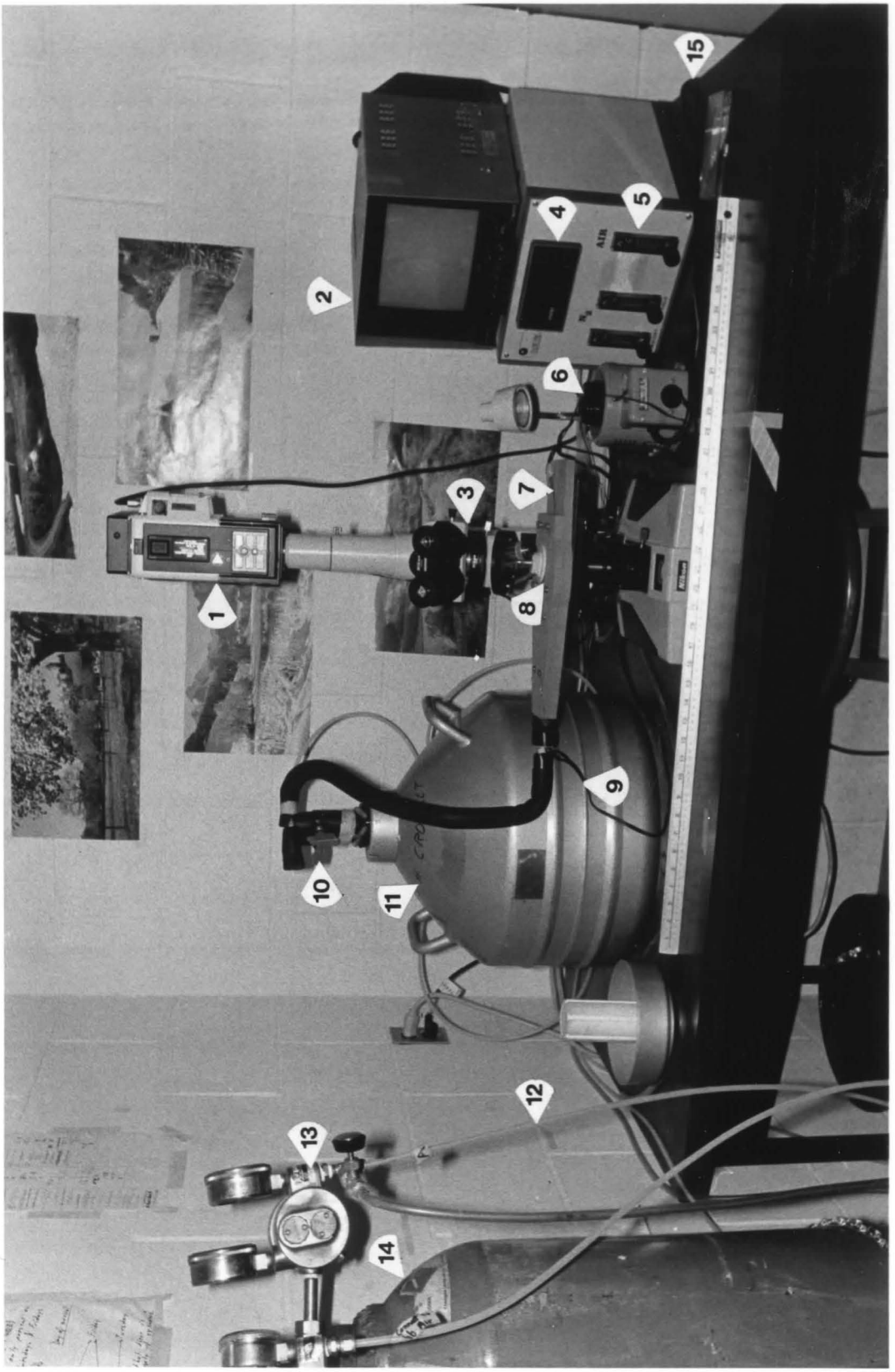

Figure 14

Chapter 3

Observations and Results

Inclusion Slides (3.1)

Inclusion slides were prepared from quartz veins and greywackes from Harrigan Cove and Dufferin, respectively.

Some samples were taken from a series of auriferous quartz veins which intruded the host rock at distinct stratigraphic layers (eg. between A and E divisions of the Bouma sequence). Other samples were cut from greywacke beds which consisted of porphyroblastic arsenopyrite and a quartz-beard that surrounded the phenocryst.

Quartz Vein Slides (3.1)

The quartz-vein samples labelled 1Q, 3Q, 4QB, 6Q1, 7A, 8A, 9Q and NW1Q2 are located on Figure 4. The first number on each sample represents the stratigraphic horizon in which the sample was collected. All quartz-vein slides were cut from the Central South pit, except sample NW1Q2, which was cut from the North West pit. These samples represent subparallel veins, except 6Q1, which is an offshoot, from the main quartz vein, crosscutting the bedding (see Fig. 4).

The quartz veins consist of quartz (85-90%), carbonate (5%) and arsenopyrite (1-10%) arranged with a crystalloblastic fabric (see Fig. 15). The quartz grains range in size from 1 to 9 mm and exhibited weak undulatory extinction. The arsenopyrite grains have a linear shape ranging in length from 1 to 5 mm. Also, they displayed a sequential fabric relative to the quartz grains. Moreover, the arsenopyrite grains exhibited a nematoblastic texture.

Quartz Beard Slides (3.3)

The quartz-beard slides, labelled 3, 6 and 12, were cut from the surrounding greywacke beds of the Central South pit of the Harrigan Cove gold district. Again, the numeric labels represents the horizon from which the sample was collected (see Fig. 4).

These samples consist of arsenopyrite porphyroblasts, pressure shadows and a matrix of quartz, feldspar and micas.The small (0.5-1mm) quartz, feldspar and micaceous minerals constitute the greywacke beds. The arsenopyrite grains range in size from 0.2 to 1.5 cm and are euhedral in shape. These porphyroblasts show neither strain nor rotation. The adjacent pressure shadows, or quartz-beards, are comprised of quartz (95%) and plagioclase (5%). The grain's length is perpendicular to the deformational stresses that were exerted at the time of growth. And they are no longer than 2.5 mm in length. The quartz grains show weak to no undulatory

extinction and no twinning was observed in the plagioclase (see Fig. 16).

In sample 12, quartz-filled fractures perpendicularly cut the foliation of the rock. Also, these micro-quartz veins appear to cross-cut the quartz-beards, but further examination reveals that the original texture of the pressure shadow remains and only along the contacts between the pressure shadow and micro-quartz vein is there any randomization of crystal growth (see Fig. 16).

Bedding-Parallel Quartz Vein Slide 3Q

Note: weakly aligned arsenopyrite grains.

non-polarized picture

Legend

QTZ...quartz

ASP...arsenopyrite

V...void space

Figure 15a

Bedding-Parallel Quartz Vein Slide 9Q

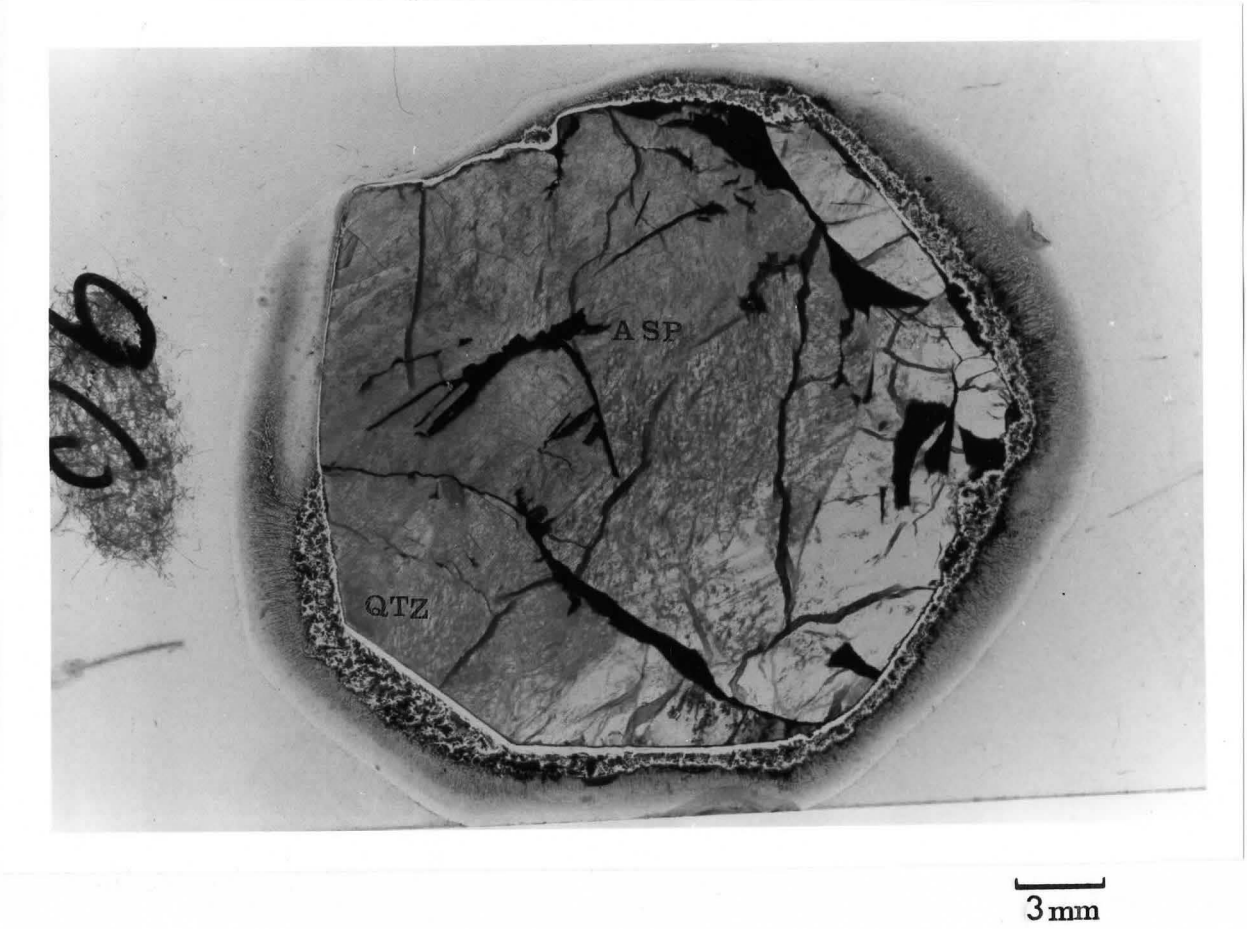

Note: non-polarized picture

Figure 15b

Bedding-Parallel Quartz Vein Slide 4QB

Note: picture taken at cross-nicols.

Figure 15c

Bedding-Parallel Quartz Vein Slide NW1Q2

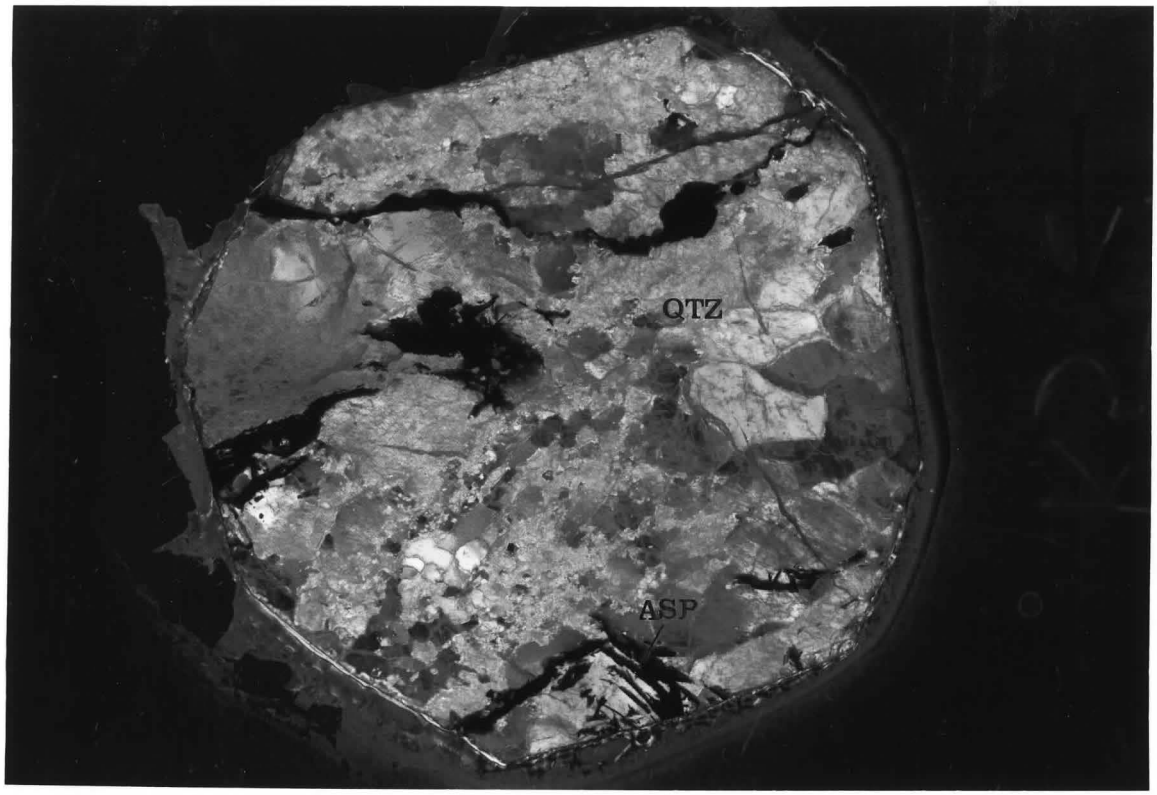

Note: picture taken with cross-nicols

Figure 15d

Bedding-Parallel Quartz Vein Slide 8A

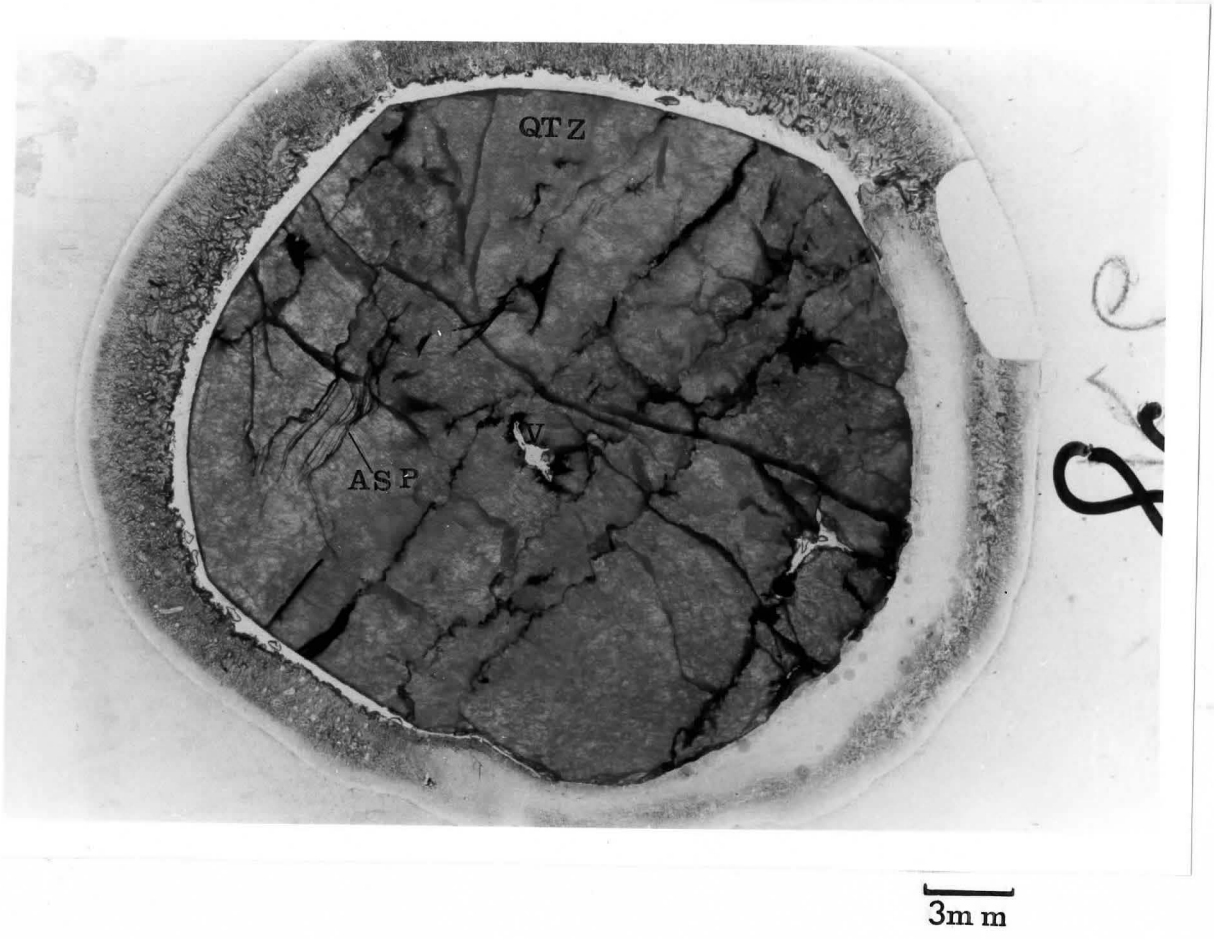

Note: non-polarized picture

Figure 15e

Quartz-Beard Inclusion Slides 3,6 and 12

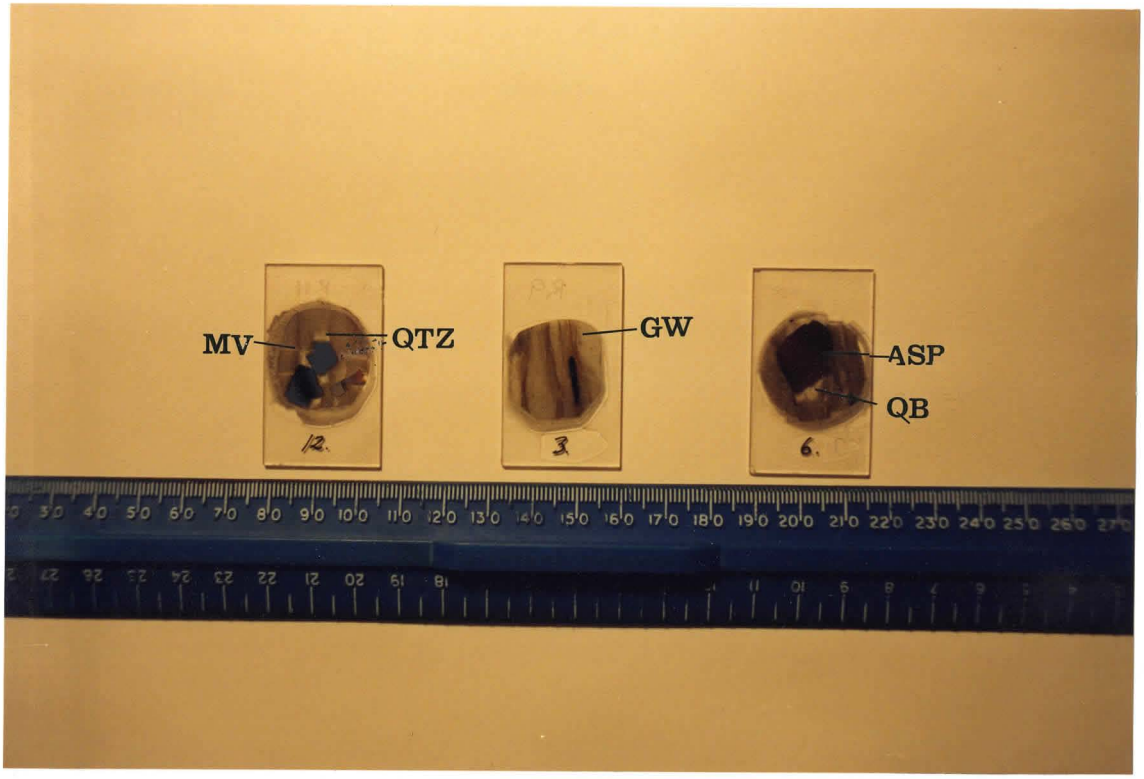

Legend

QTZ...quartz

ASP...arsenopyrite

GW...fine matrix material

MV...micro-quartz vein

QB...quartz-beard

Figure 16

Fluid Inclusions (3.4)

The inclusions studied were from quartz crystals, which occur in the quartz-veins (samples 1Q, 3Q, 4QB, 6Q1, 7A, 8A, 9Q and NW1Q2). No inclusion work was permissible on the quartz-beard samples; this was the result of the inclusions found in these samples being too small for any accurate measurements to be taken.

Firstly, all inclusions, to be studied, were categorized as either primary/secondary or pseudo-secondary. The grouping of primary and secondary inclusions was necessary, because their morphologies were very similar.

Primary/secondary inclusions were characterized as having (see Fig. 17):

i) irregular, tubular or oblate shapes,

ii) random fluid-fill,

iii) size varying from <5 microns to 120 microns, and

iv) necking down edges (characteristically S-inclusion).

Pseudo-secondary inclusions were much more easily identified. The characteristics used to recognize a PS-inclusion were (see Fig. 18):

i) tubular to oblate in shape,

ii) fluid-fill is approximately 70%.

iii) aligned in linear paths, and

iv) an average size of 40 microns.

Primary/Secondary Fluid Inclusions

in Quartz Crystals

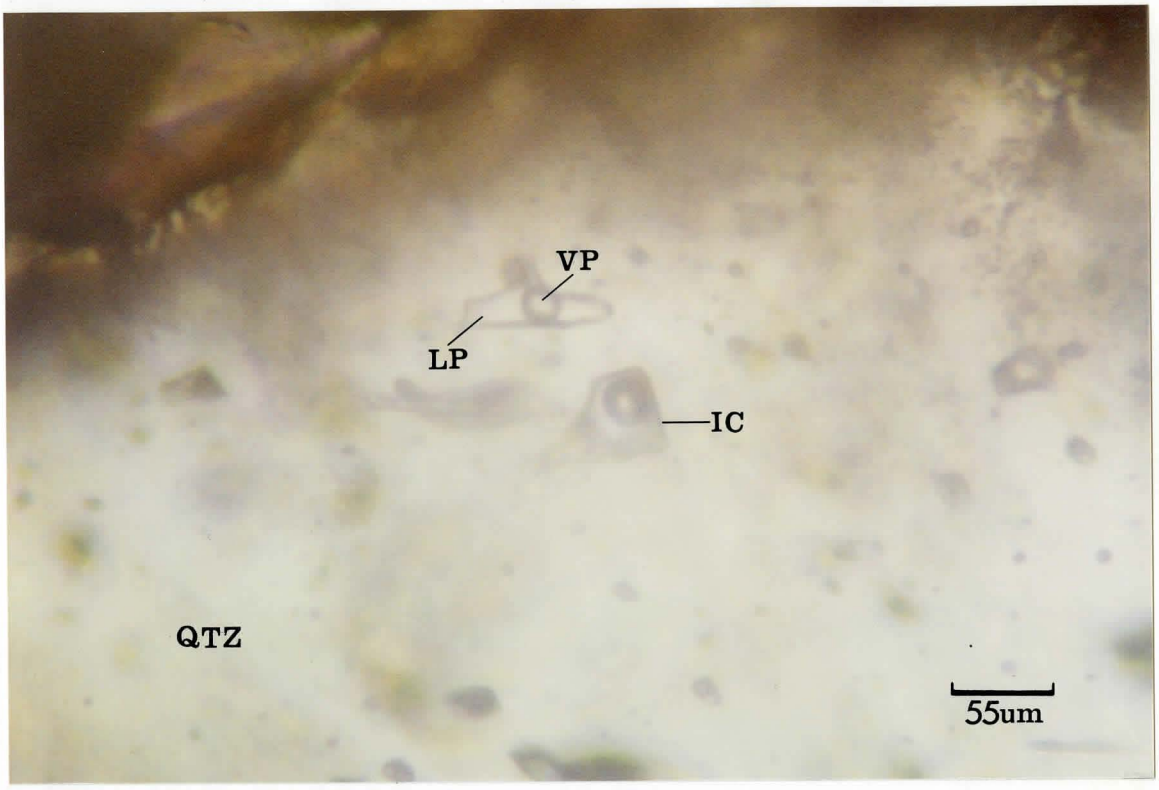

Note: the tubular shape of inclusion 1 and the smaller fluid-fill in 2.

Legend

IC...inclusion cavity

VP...vapour phase(bubble)

LP...liquid phase

QTZ..quartz

Figure 17a

Primary/Secondary Fluid Inclusions

in Quartz Crystals

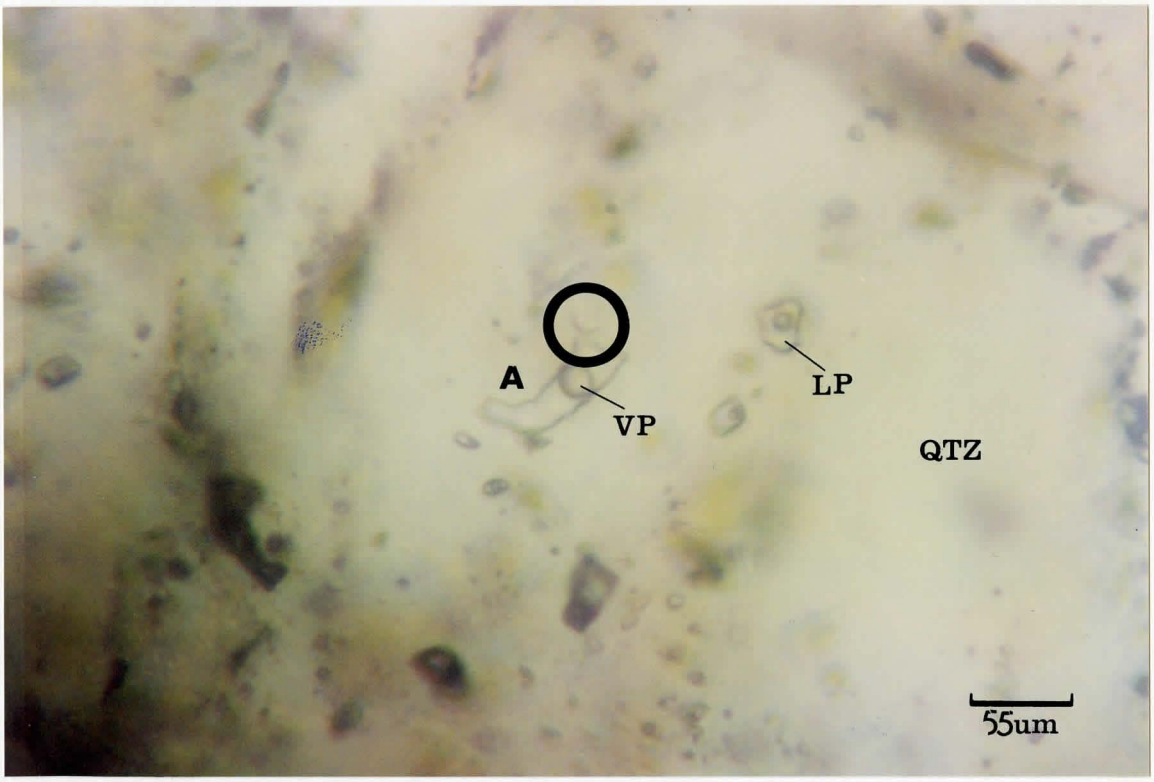

Note: the rectangular shape and the difference in sizes. Again, the fluid-fill is random. Inclusion A shows

Figure 17b

Primary/Secondary Fluid Inclusions

in Quartz Crystals

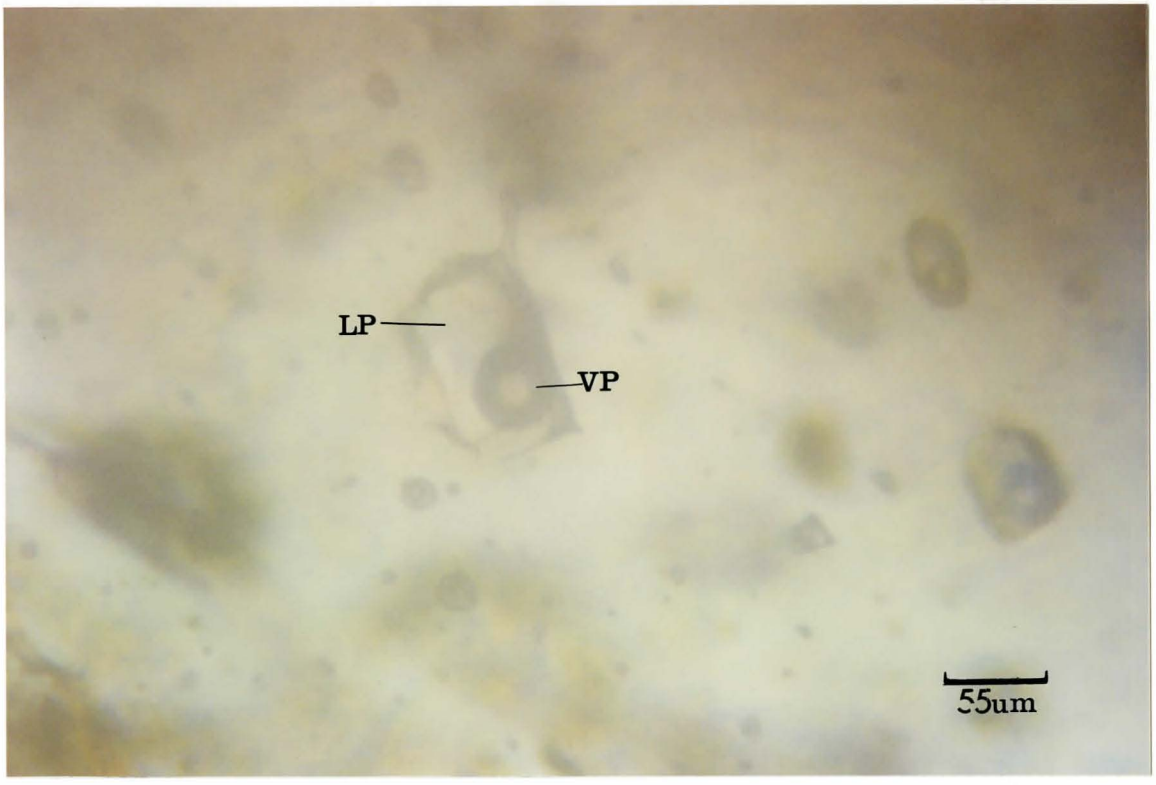

Note: the random size and shape.

Figure 17c

Primary/Secondary Fluid Inclusions

in Quartz Crystals

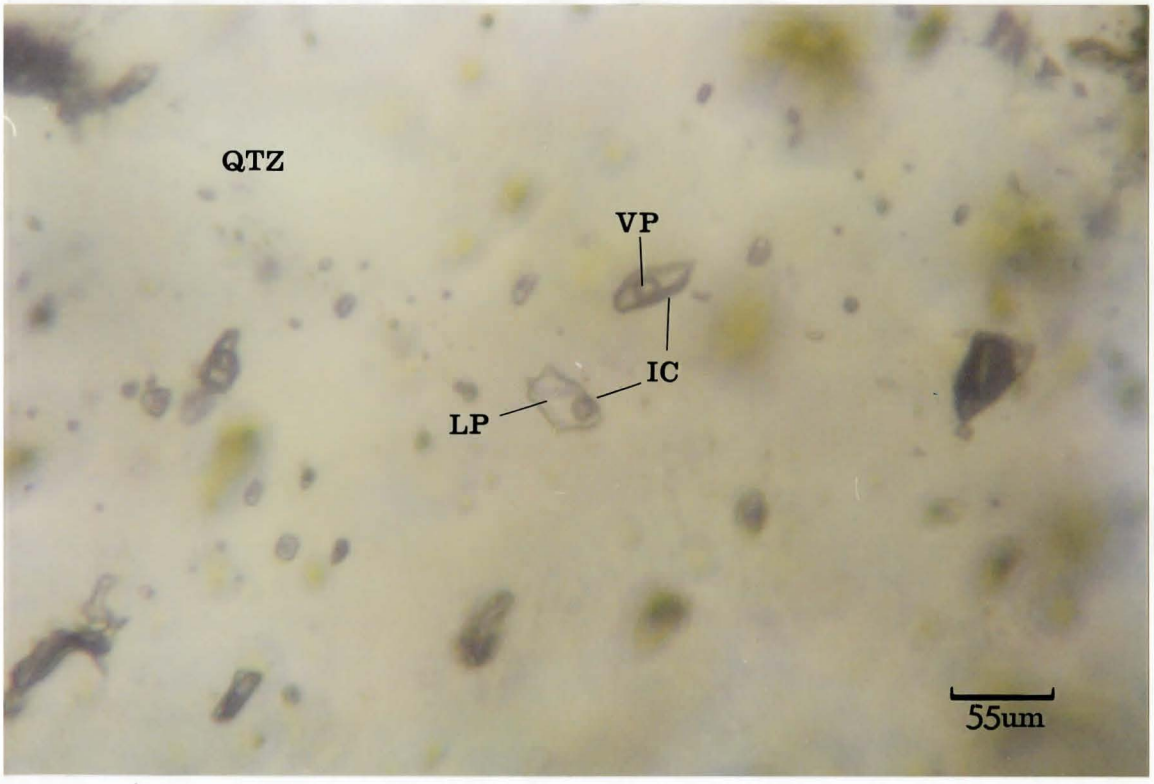

Figure 17d

Pseudo-Secondary Fluid Inclusions

in Quartz Crystals

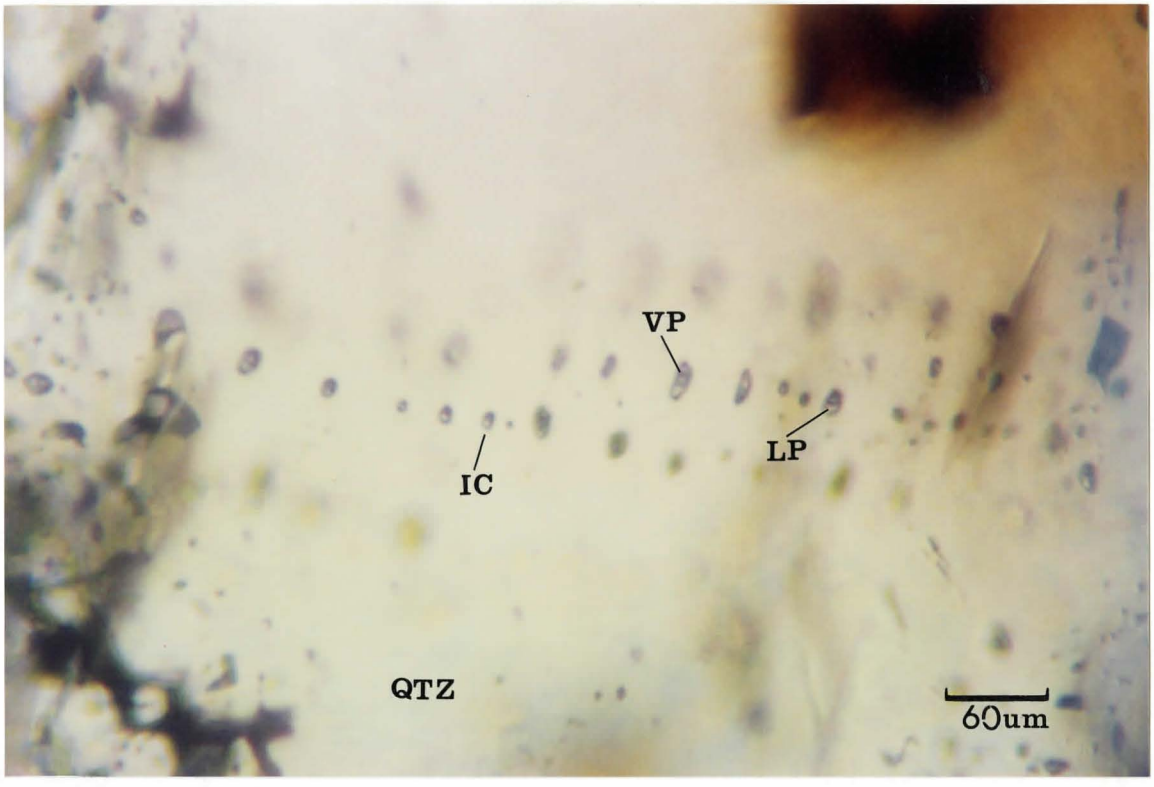

Note: the alignment of inclusions which is indicative of PS-inclusions. Also, the constant fluid-fill. Moreover, the shapes are oblate to tubular and size is relatively consistent.

legend

VP...vapour phase(bubble)

LP...liquid phase

IC...inclusion cavity

QTZ..quartz

Figure 18a

Pseudo-Secondary Fluid Inclusions

in Quartz Crystals

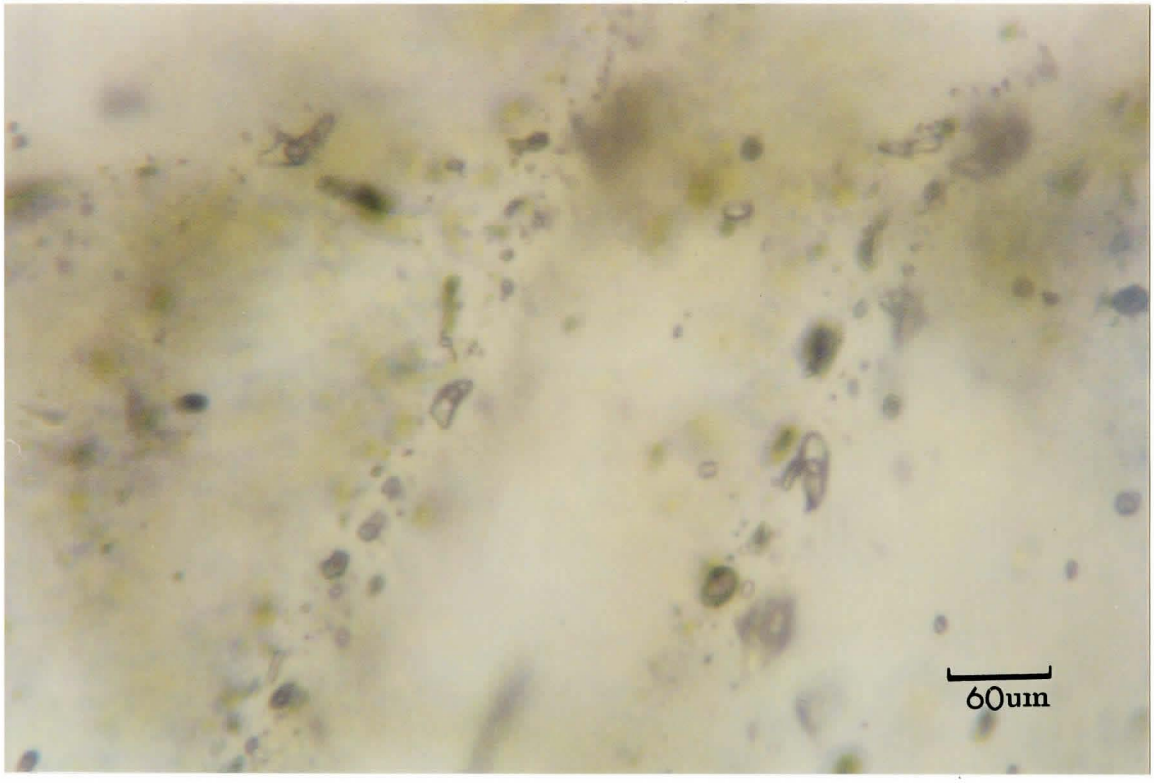

Figure 18b

Pseudo-Secondary Fluid Inclusions

in Quartz Crystal

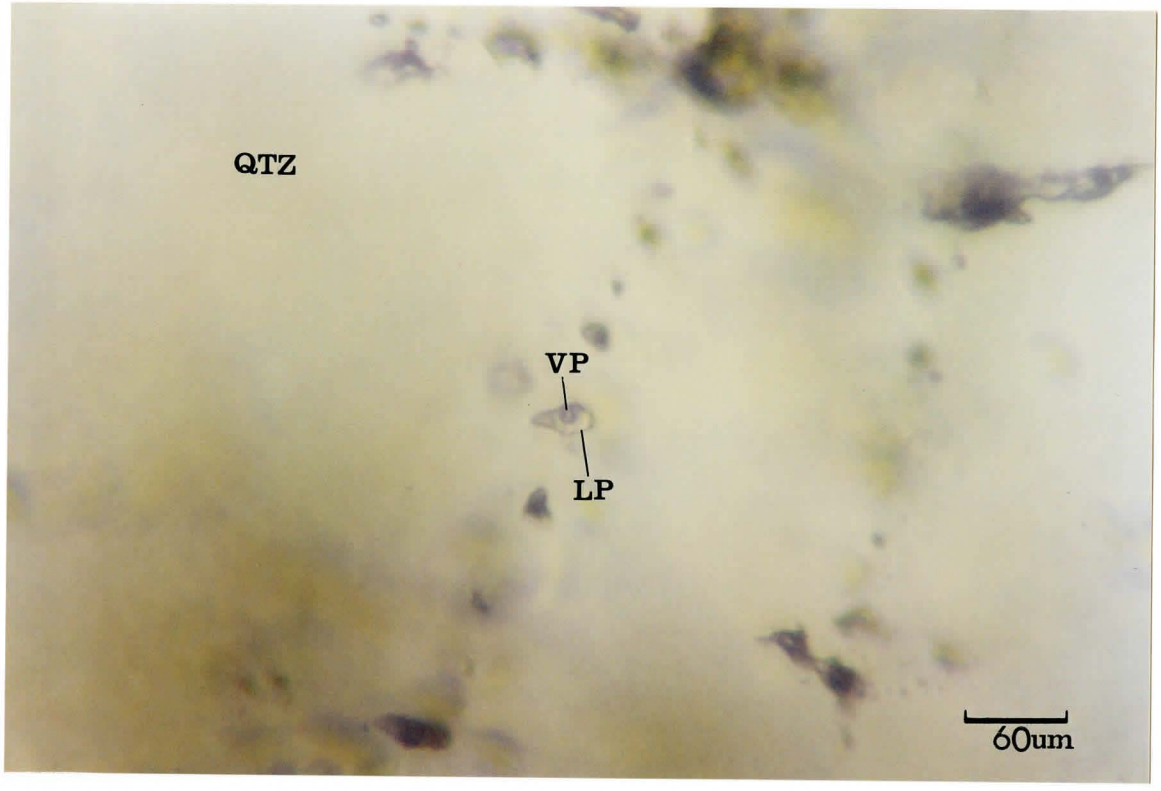

Figure 18c

Collected Data (3.5)

A total of over 90 inclusions were observed for homogenization and first-melt temperatures. The following tables are given to illustrate the collected data. Two phase column represents temperature of first appearance of vapour bubble on cooling.

TABLE 2

Homogenization Temperatures of Primary/Secondary Inclusions From Harrigan Cove, Nova Scotia

	Temperature (Celsius)	
Sample No.	Homogenization	Two Phase
1Q	314.6	301.2
1Q	239.9	-----
1Q	325.6	318.3
1Q	365.0	342.0
1Q	388.3	-----
3Q	249.0	-----
3Q	326.8	318.9
3Q	318.0	295.4
3Q	338.5	331.0
4QB	375.6	363.8
4QB	304.7	292.5
4QB	279.4	-----
6Q1	275.4	254.0
6Q1	322.3	-----
6Q1	354.2	350.8

(...continued)

6Q1	350.2	-----
6Q1	275.8	263.7
6Q1	319.7	269.2
6Q1	277.6	259.5
6Q1	259.0	210.8
6Q1	291.8	268.1
6Q1	255.6	-----
6Q1	349.6	328.3
7A	376.7	372.4
7A	315.2	305.0
7A	314.6	306.2
7A	330.1	327.7
7A	385.9	376.2
7A	297.5	282.2
7A	306.6	291.7
7A	349.7	-----
7A	330.6	-----
7A	302.0	-----
8A	308.6	302.9
8A	353.4	345.0
9Q	242.5	-----
9Q	262.5	-----
9Q	270.0	-----
9Q	320.9	-----
9Q	363.5	-----

(...continued)

9Q	345.5	-----
NW1Q2	283.6	281.0
NW1Q2	236.2	227.0
NW1Q2	263.3	-----

Table 3

Homogenization Temperatures of Pseudo-secondary Inclusions From Harrigan Cove, Nova Scotia

	Temperature (Celsius)	
Sample No.	Homogenization	Two Phase
3Q	279.7	-----
4QB	259.7	-----
4QB	265.3	249.2
4QB	275.6	234.7
4QB	286.0	-----
4QB	290.0	253.7
6Q1	276.0	-----
6Q1	275.6	260.9
7A	329.6	288.0
7A	306.4	280.0
7A	300.9	280.0
7A	309.6	306.0
NW1Q2	266.2	-----
NW1Q2	270.8	-----

(...continued)

NW1Q2	282.3	-----
NW1Q2	277.7	-----
NW1Q2	280.6	-----

Table 4

First- and Last-Melt Temperatures of Primary/Secondary Inclusions From Harrigan Cove, Nova Scotia

	Temperature (Celsius)	
Sample No.	First-Melt	Last-Melt
1Q	-32.7	-4.0
1Q	-35.7	-4.0
1Q	-32.5	----
3Q	-32.5	----
3Q	-34.7	-3.5
3Q	-33.8	-1.7
4QB	-34.8	-5.5
4QB	-34.9	----
4QB	-36.7	-3.4
4QB	-33.9	----
6Q1	-37.0	-4.2
7A	-34.0	----
7A	-37.0	----
7A	-37.2	----
7A	-34.7	-2.0

(...continued)

7A	-38.2	-3.1
8A	-35.0	-4.9
8A	-32.7	----
8A	-34.0	-3.0
NW1Q2	-35.0	-2.7

Table 5

First- and Last- Melt Temperatures of Pseudo-secondary Inclusions From Harrigan Cove, Nova Scotia

	Temperature (Celsius)	
Sample No.	First-Melt	Last-Melt
3Q	-33.0	----
3Q	-30.0	-2.0
3Q	-31.8	-4.8
3Q	-28.0	-4.3
4QB	-29.0	-3.7
4QB	-24.4	-0.8
6Q1	-32.0	-1.4
6Q1	-28.6	-3.0
8A	-28.0	----
8A	-26.0	-2.7
8A	-29.9	----
NW1Q2	-28.4	----
NW1Q2	-27.9	----

Calculations (3.6)

The number of homogenization temperatures (T_H) of primary/secondary and pseudo-secondary inclusions from Tables 2 and 3 is 44 and 17, respectively. Using simple statistical calculations mean and standard deviation can be derived. Thus,

T_H for P- and S-inclusions is 311.7°C +/- 41.7°C, and

for PS-inclusions is 284.2°C +/- 18.1°C.

*Note- the large standard deviation for P/S-inclusions is the result of the grouping together of the two distinct inclusion types.

The first-melt temperature (T_F) for both primary/secondary and pseudo-secondary inclusions can be derived by statistical means as well. Using the data from Tables 4 and 5 for P/S- and PS-inclusions, respectively, the means are:

T_F for P/S-inclusions is -32.7°C +/- 3.7°C, and

for PS-inclusions is -32.1°C +/- 3.1°C.

The number of data for P/S- and PS-inclusions is 22 and 13, respectively.

The first-melt or eutectic temperature for both primary/secondary and pseudo-secondary is relatively equal. Thus, the salt content within the inclusions is considered to be the same. But, some deviation may be present in the secondary inclusions which have been grouped with the primary inclusions.

This eutectic temperature corresponds within one standard deviation of the $MgCl_2$-H_2O salt system (see Table 6). Knowing the salt present within the fluid of the inclusion the density of the fluid can be derived by optical examination of the vapour phase present and the fluid-fill. Thus,

$$P_T = P_L \times F + P_V(1-F) \quad \text{(eq.2)}$$

,where P_T is total density of inclusion

P_L is density of liquid phase

P_V is density of vapour phase

F is degree of fill

but $P_T = P_L \times F$ (eq.3), since the density of the vapour phase is neglible. And total density is derived by knowing the weight percent of $MgCl_2$ in solution.

With the aid of Graph 2, the weight percent salt in solution is extrapolated from the freezing point depression value, which is the eutectic temperature measured from the inclusions. Thus, 21.25 wt% $MgCl_2$ is present in solution. Therefore, the total density of the inclusion is estimated from Graph 3 to be 0.85g/cm^3. Incorporating total density and degree of fill (0.7) into equation 2, the density of the liquid phase is calculated to be 1.21g/cm^3.

Table 6

Table of Salt Systems with Corresponding Eutectic Temperatures

Salt system	Eutectic temperature (°C)	Solid phases
H_2O–NaCl–$CaCl_2$	−55	ice + $NaCl.2H_2O$ + $CaCl_2.6H_2O$
	(−52)	
H_2O–$MgCl_2$–$CaCl_2$	−52.2	ice + $MgCl_2.12H_2O$ + $CaCl_2.6H_2O$
*H_2O–KCl–$CaCl_2$	−50.5	ice + $CaCl_2.6H_2O$
H_2O–$CaCl_2$	−49.5	ice + $CaCl_2.6H_2O$
H_2O–Na_2CO_3–K_2CO_3	−37.0	ice + $(K,Na)_2CO_3.6H_2O$ + $K_2CO_3.6H_2O$
H_2O–NaCl–$FeCl_2$	−37.0	ice + $NaCl.2H_2O$ + $FeCl_2.6H_2O$
H_2O–$FeCl_2$	−35.0	ice + $FeCl_2.6H_2O$
H_2O–NaCl–$MgCl_2$	−35.0	ice + $NaCl.2H_2O$ + $MgCl_2.12H_2O$
H_2O–$MgCl_2$	−33.6	ice + $MgCl_2.12H_2O$
*H_2O–NaCl–KCl	−23.5	ice + $NaCl.2H_2O$
	(−22.9)	
H_2O–NaCl–Na_2SO_4	−21.7	ice + $NaCl.2H_2O$ + $Na_2SO_4.5H_2O$
H_2O–NaCl–$NaHCO_3$	−21.8	ice + $NaCl.2H_2O$ + $NaHCO_3$
H_2O–NaCl–Na_2CO_3	−21.4	ice + $NaCl.2H_2O$ + $Na_2CO_3.10H_2O$
H_2O–NaCl	−21.2	ice + $NaCl.2H_2O$
	(−20.8)	
*H_2O–KCl	−10.6	ice
H_2O–$NaHCO_3$–Na_2CO_3	−3.3	ice + $NaHCO_3$ + $Na_2CO_3.10H_2O$
H_2O–$NaHCO_3$	−2.3	ice + $NaHCO_3$
H_2O–Na_2CO_3	−2.1	ice + $Na_2CO_3.10H_2O$
H_2O–Na_2SO_4	−1.2	ice + $Na_2SO_4.10H_2O$

(Shepherd et al., 1986)

Graph of Freezing Point Depression versus

Weight Percent Salt in Solution

for typical Inclusion Salts

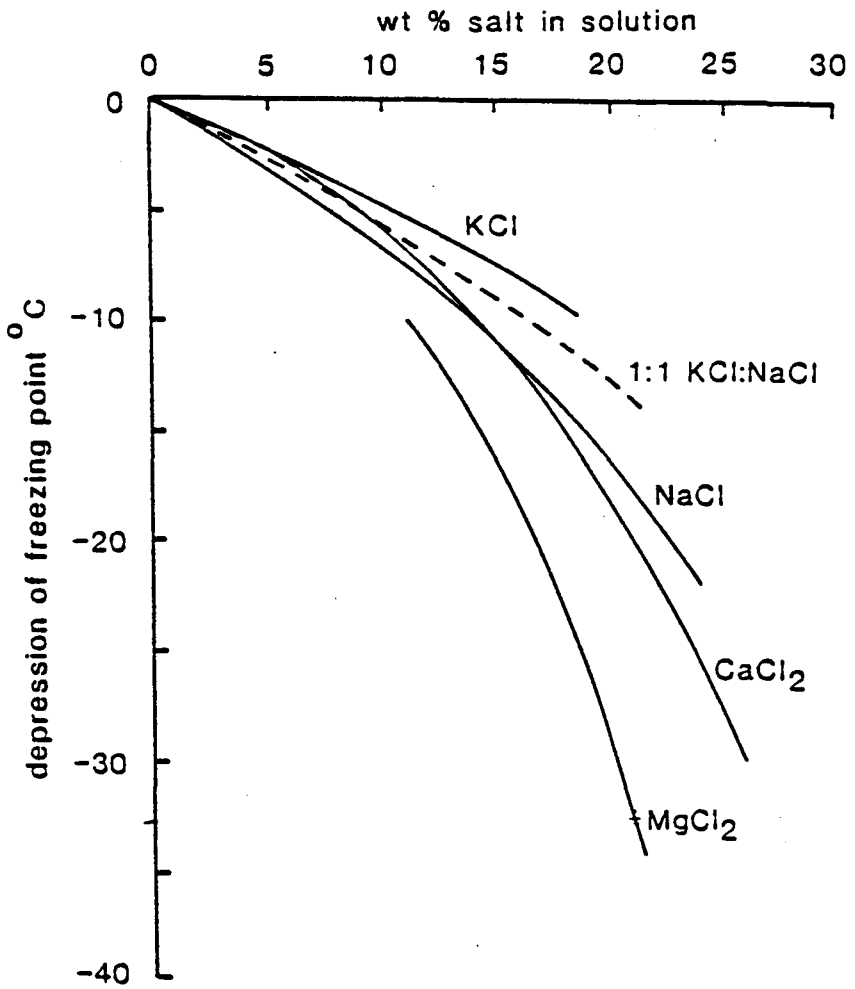

Graph 2 (Shepherd et al., 1986)

Degree of Fill versus Weight Percent

Salt in Solution

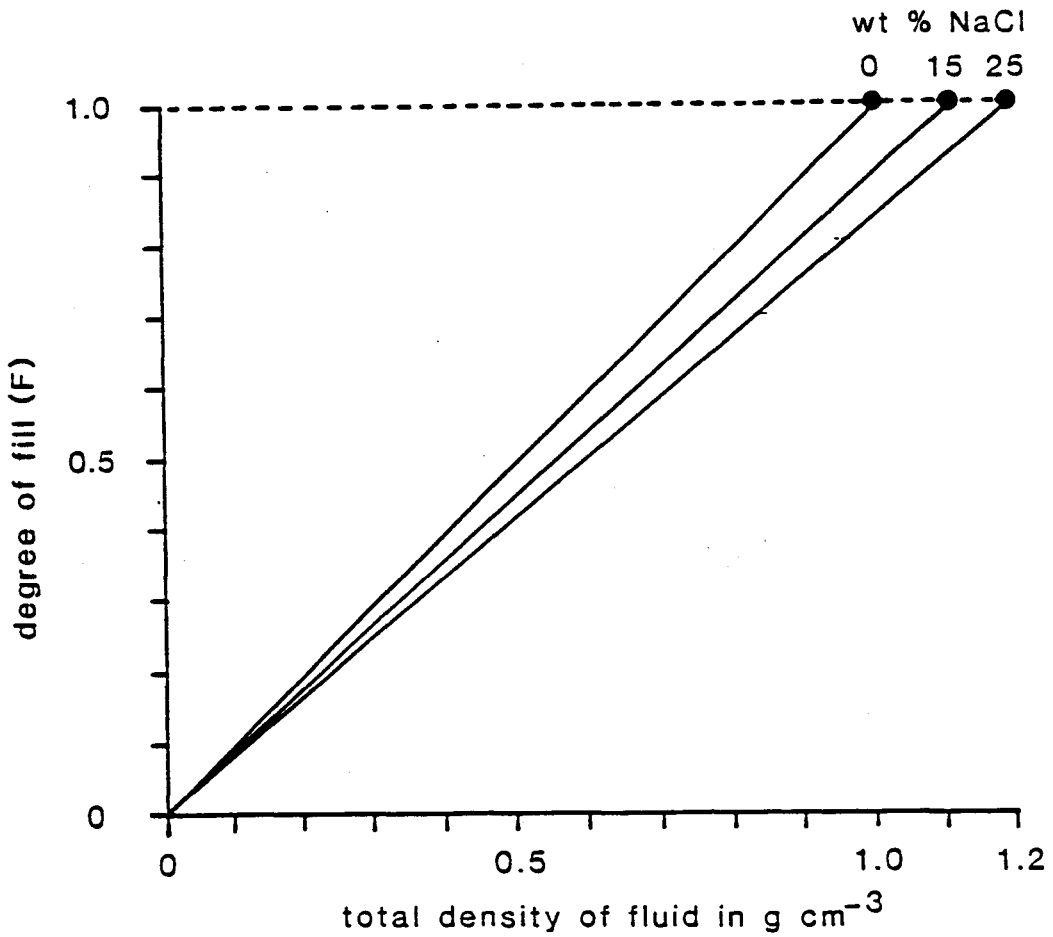

Note: for $MgCl_2$, if wt% is to the right of the eutectic it may be considered as NaCl for deriving density.

Graph 3 (Shepherd et al., 1986)

Homogenization Temperatures of Primary Pseudo-Secondary Inclusions From Harrigan Cove, Nova Scotia

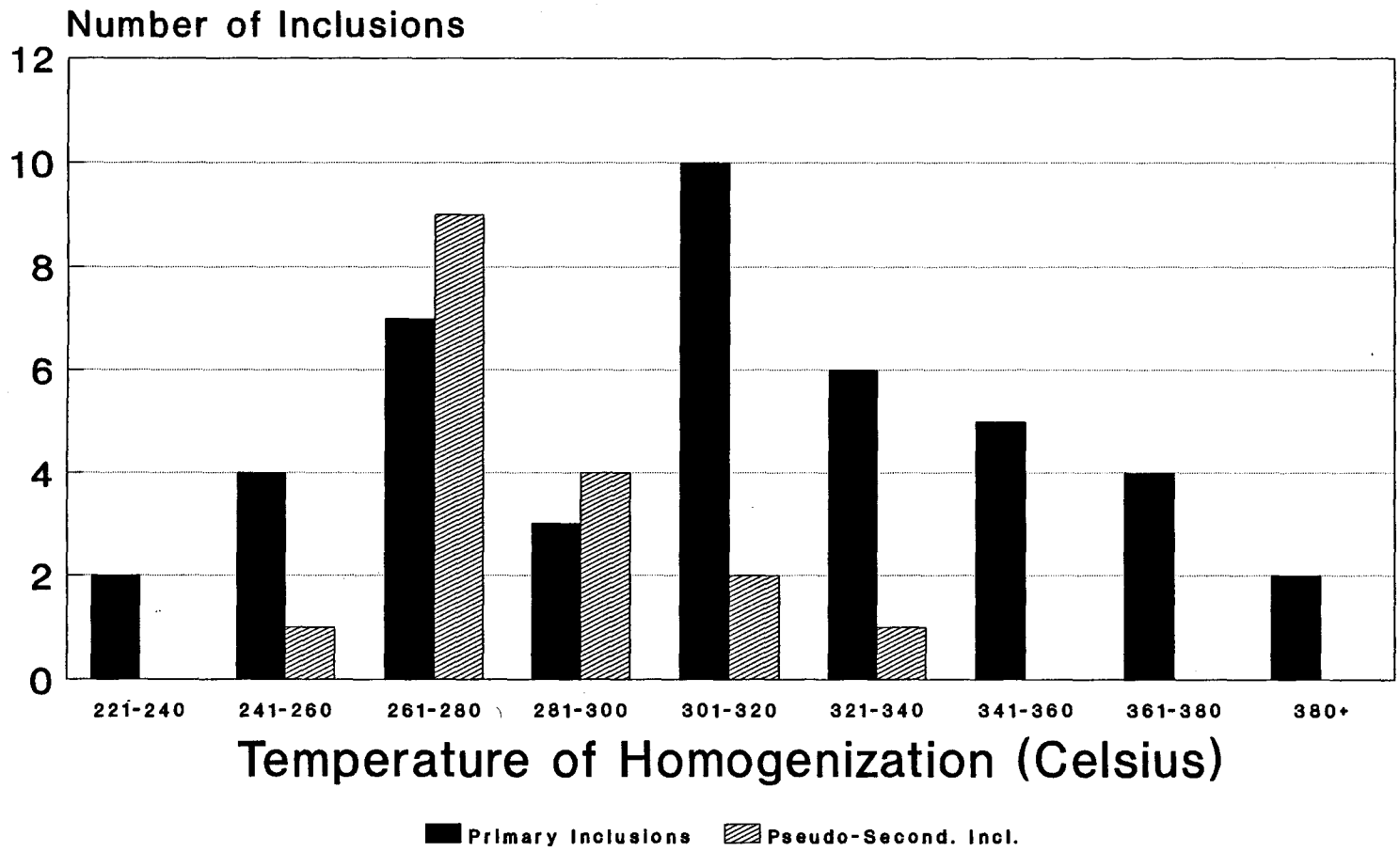

Graph 4

First-Melt Temperatures of Primary and Pseudo-Secondary Inclusions From Harrigan Cove, Nova Scotia

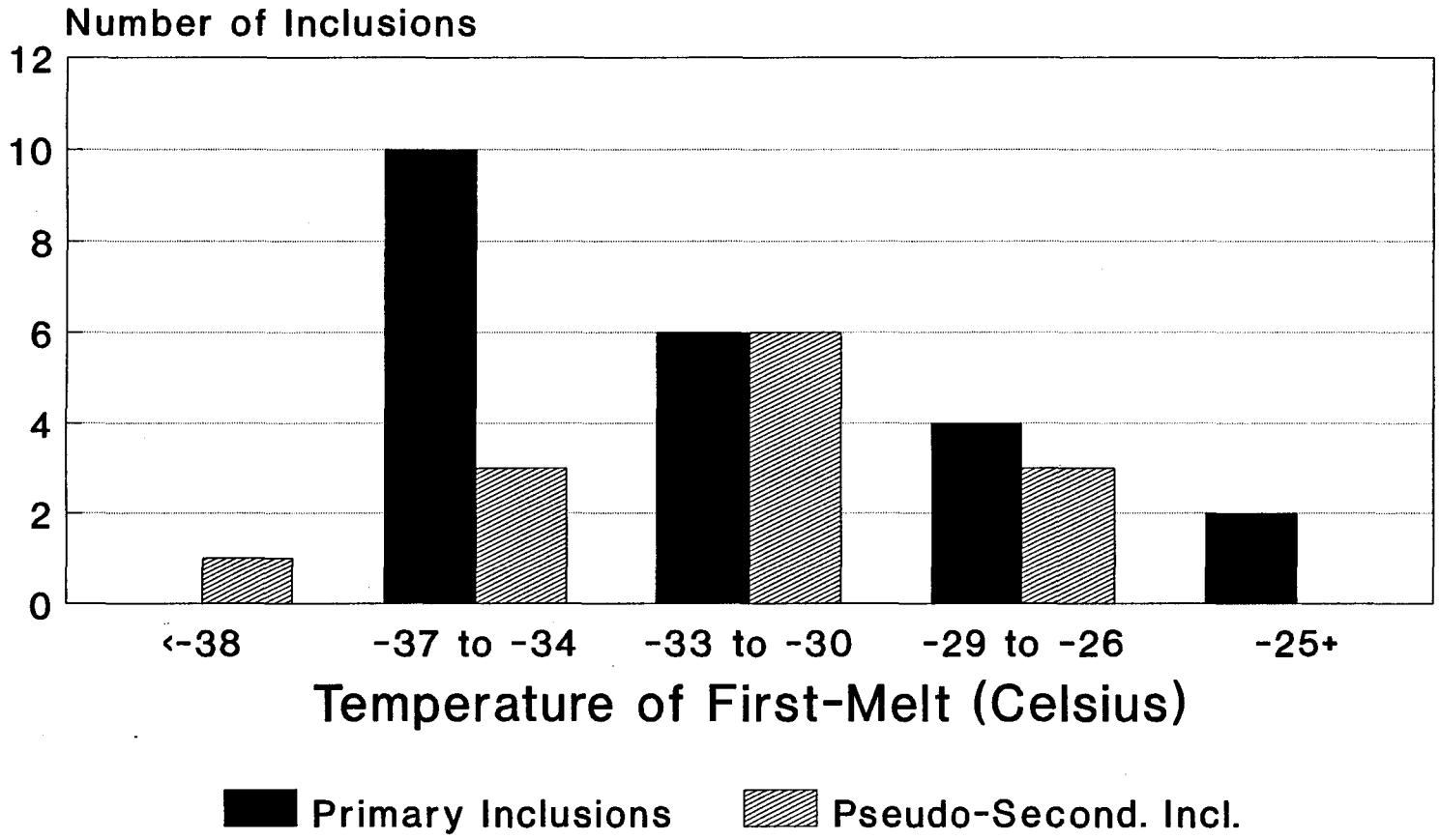

Graph 5

Phase Diagram for $MgCl_2$ - H_2O System

From Harrigan Cove, Nova Scotia

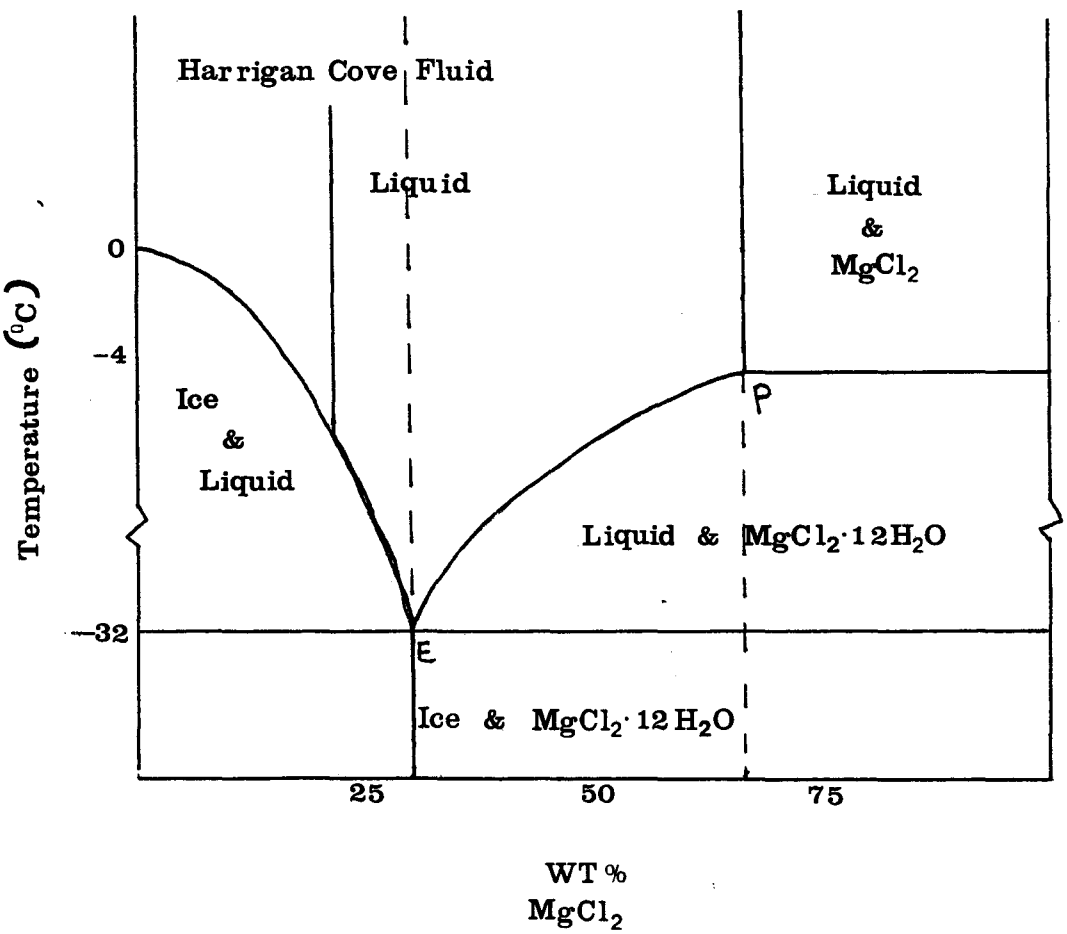

Graph 6

Log aO_2 - pH Diagram Illustrating Regions of Gold Solubility

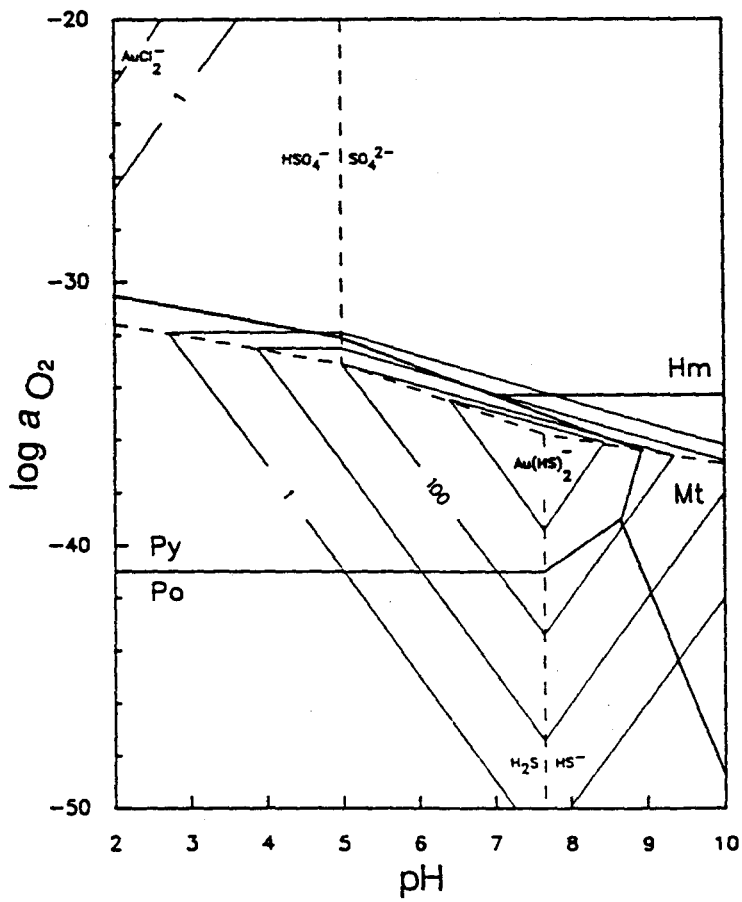

Graph 7 (Schenberger and Barnes, 1989)

Table 7

Average Metal and CO_2 Contents by Area and Lithology, Harrigan Cove, Nova Scotia

Average metal and CO_2 contents by area and lithology at Harrigan Cove.

Area	Average Metal and CO_2 Contents in A, E and Q units														
	Au, ppb			As, ppm			Sb, ppm			CO_2, wt.%			Number of samples for each locality		
	A	E	Q	A	E	Q	A	E	Q	A	E	Q	A	E	Q
N & NW	19	24	6.4	4203	2823	167	14	17	1.5	.30	.26	.13	6	3	6
CN	6.1	8.0	14	945	228	142	7.4	2.8	1.8	.19	.28	.14	2	6	5
CS	6.0	4.8	14	1350	152	277	6.0	1.9	1.9	.33	.33	.12	18	14	10
S	21	23	289	21	86	44	0.71	1.0	1.0	.51	.23	.12	6	6	4

(Crocket et al.,1986)

Chapter 4

Discussion

Fluid Inclusion Data Interpretation (4.1)

Homogenization temperatures for primary/secondary and pseudo-secondary inclusion from Tables 2 and 3, respectively, are plotted on Graph 4. The histogram reveals a possible bimodal relationship for the primary/secondary inclusion family. This relationship can be explained by the necessary grouping together of the two types of inclusions. The higher temperature Gaussian curve is skewed to the left, this may be illustrative of a minimum trapping temperature of primary inclusions at approximately 301°C. The lower temperature curve may be interpretated as the sealing temperatures of the secondary inclusions which form after crystallization is complete.

For the pseudo-secondary inclusions Graph 4 illustrates a Gaussian curve skewed also to the left. Again, a large majority of this type of inclusion were trapped at a minimum temperature of approximately 261°C. The pseudo-secondary inclusions are representative of the fluids which entered the veins by hydraulic fracturing (Graves and Zentilli, 1982). Thus, the vein forming fluids of the Meguma rocks are low temperature.

A histogram was also plotted for first-melt temperatures (see Graph 5) using the data from Tables 4 and 5. Here both primary and pseudo-secondary inclusions show similar first-melt temperatures. This may indicate that the salt content of the fluids within the inclusions are similar if not identical. The higher temperature readings on Graph 5 may be the result of secondary inclusions which were grouped with the primary inclusions. The secondary inclusions perhaps have a different salt content than the other two inclusion types. A more Na-rich salt is suggested for the secondary inclusions or at least some other univalent cation. Most univalent cation salt solutions have first-melt temperatures in the low to mid negative twenty degree range, whereas divalent cation salt solutions have first-melt temperatures at least ten degrees lower than their univalent counterparts.

The salt content of the fluids found within the inclusions of the Meguma veins was derived to be $MgCl_2$ (see Chapter 3). The weight percent of the salt was calculated to be 21.25wt% $MgCl_2$. This value plots to the left of the eutectic on Graph 6 suggesting that no daughter minerals within the inclusions are present; this is indeed what was observed. Values to the right of the eutectic on Graph 6 are only hypothetical.

Also, the density of the liquid phase was calculated to be $1.21 g/cm^3$ (see Chapter 3).

Ligand Complexes (4.2)

In aqueous solutions the dominant oxidation species of gold is Au(III) with lesser concentrations of Au(I) (Seward, 1991). In these two oxidation states gold can be mobilized (complexed) by at least two ligand complexes, sulphide and chloride (Shenberger and Barnes, 1989). The sulphide and chloride ligands are most stable with gold as the complexes $Au(HS)^-_4$ and $AuCl^-_4$, and to a lesser extent $Au(HS)^-_2$ and $AuCl^-_2$, respectively (Seward, 1991).

Seward(1991) states that sulphur is present primarily in the negative 2 oxidation state (sulphide ion) in most hydrothermal ore solutions where low oxidation potential prevails. Also, the high stability of gold in a complex with a reduced sulphur ligand permits easy transportation of gold in hydrothermal solutions. Shenberger and Barnes (1989) illustrated the high solubility of gold in near neutral to alkaline pH and high sulphur content. These observations can be used to model gold transport for the Meguma rocks.

The presence of arsenopyrite (see Fig.15 and 16) in the Goldenville Formation is evidence for a sulphur concentration large enough to mobilize gold. The lack of brittle deformation of these grains suggests that they crystallized synchronously with gold. The co-precipitation of a sulphide mineral along with gold may reflect a high arsenic content carried by fluids with synchronous precipitation of arsenic and gold through a REDOX reaction.

Chloride is a second ligand that may complex with gold but gold-chloride complexes are not as dominant as hydrosulphide (Shenberger and Barnes, 1989). If Cl^- concentrations are high enough chloride complexes with gold become more important. Reasoning that there was sufficient chlorine ions to bond with magnesium inferred from the fluid inclusion freezing point data and that no other univalent cation species were present a large concentration of Cl^- is hypothesised. This ligand was probably available to complex with gold as it traversed the host rock.

The most stable gold chloride complex is $AuCl^-_4$ according to Seward (1991), but Uematsu and Franck (1980) pointed out that at high temperatures and with excess chloride ligands, $AuCl^-_2$ is more stable and behaves as the major gold mobilizer. However, the suggested fluid temperatures of 260°C to 300°C for Meguma vein fluids is much lower than the temperatures suggested by Uematsu and Franck (1980) for significant $AuCl^-_2$.

From observations made on the inclusions, no daughter minerals were found, therefore, the fluids were not saturated with magnesium chloride salt. This is illustrated on Graph 6 which shows a first-melt temperature of -32°C so that Meguma vein fluids had a composition left of the eutectic.

Source of Ligands (4.3)

The paleo-environment inferred by deposition of off-shelf turbidites such as the Meguma sediments would be a deep-sea setting and the incorporation of sea water under low oxygenation and broadly reducing conditions seems likely. Schenk (1970) and others have also suggested a deep-sea environment. Thus, naturally occurring, sea-water salt could accumulate, therefore, increasing the concentration of the potential chloride ligands.

Gold Mobilization (4.4)

Solutions containing reasonable concentrations of reduced sulphur and chloride can transport significant quantities of gold. The chemical conditions under which substantial quantities of gold may be transported are illustrated in Graph 7. The field where gold is highly soluble as $Au(HS)^-_2$ and $AuCl^-_2$ is largely coincident with the pyrite and hematite fields, respectively, depending on availability of iron. Thus, pyrite and hematite should precipitate along with gold in such a hydrothermal deposit. But, within the Meguma Group there is no pyrite and very little hematite.

The lack of either pyrite or hematite in the Meguma rocks may be the result of low concentrations of sulphur and iron. Though the sulphide concentration is large enough to transport parts-per-billion quantities of gold it is not sufficient to precipitate pyrite, which requires two sulphurs for every iron cation. On the other hand,arsenopyrite a mineral with lower mole fraction sulphur than pyrite has formed. A possible source of iron in Meguma vein fluids is from the metamorphic degradation of biotite and chlorite. Thus, the biotite which formed during the greenschist metamorphic event may have been destroyed by the fluids that traversed the host rock picking up gold cations.

Shenberger and Barnes (1989) explained the different depositional mechanisms for gold complexed with hydrosulphide and chloride ligands. For the Meguma gold deposits, deposition caused by reduction is most probable. As the ore fluid hydraulically fractured the rocks between the A and E divisions (Graves and Zentilli, 1982), the gold complexes underwent reduction as the vein fluid reacted with the hydrocarbons in the organic-rich slates.

As the complexed gold is destabilized and gold metal precipitates, the sulphide and chloride ligands acquired a new cation species. The degradation of biotite was the source for these new cations. The biotite grains would release Fe and Mg cations to freely bond with S and Cl, respectively. Since, a low concentration of S was present to begin with, pyrite precipitation was not possible. Thus, As which is strongly related to Au, bonded with Fe and S to form arsenopyrite. The released Mg cations would bond with

Cl anions to form the salt present in the fluids of the inclusions. Also, the initial concentration of Na, from cognate sea-water, would join with SiO_2 tetrahedrons to form plagioclase, which is present in the quartz beards. This whole process is dependent on the reduction (fluid reaction with hydrocarbons) shifting the sulphur equilibrium to more reducing values, so that more reduced species of sulphur become available.

Au-As Relationship (4.5)

Crocket et al.(1986) produced interelement correlation coefficients for gold, arsenic, antimony and carbon dioxide, which are summarized on Table 7. They were able to show that antimony and gold strongly correlated with arsenic in greywackes and slates and inferred that the metal probably, substituted in the structure of arsenopyrite. These correlations suggesting that gold was more strongly controlled by native gold or other sulphides in the veins. Thus, they concluded that gold distribution and concentration in slates and greywackes is controlled by arsenopyrite but not in quartz-veins.

Chapter 5

Conclusion

The Meguma rocks at Harrigan Cove, Nova Scotia, have a higher gold content than similar rocks (greywackes) in other geographic localities. From fluid inclusion data the fluids which mobilized the gold and later deposited it in bedding-parallel quartz veins and in smaller quantities in the surrounding country rock must have been a low temperature (260°C to 300°C) and sulphur concentration solution.

Also, the salt in solution is $MgCl_2$ with a weight percent of 21.25 for both primary and pseudo-secondary inclusions. The secondary inclusions with a higher first-melt temperature probably have an univalent cation salt in solution as the dominant species.

In the temperature region specified the Au cations were probably carried as $Au(HS)_4^-$ complexes with a smaller quantity mobilized as $AuCl_4^-$ complexes. As the gold-rich solutions entered the veins which were produced by hydraulic fracturing (Graves and Zentilli, 1982) the Au-complexes were reduced in a REDOX reaction with the organic-rich slates. The concentration of Au in the quartz veins is dependent on how far the reduction process developed. It is hypothesised here that this reduction process was not complete due to the small presence of gold.

References

Anderle, J.P., 1974. Geological report on the Harrigan Cove property, Halifax County, Nova Scotia. Assessment file no. 21H23 (02), Nova Scotia Department of Mines and Energy. p15.

Boyle, R., 1672. Essay about the Origine and Virtues of Gems. William Godbird. London, p185.

Boyle, R.W., 1979. The geochemistry of gold and its deposits. Geological Survey of Canada, bulletin 280:584.

----------, 1986. Gold deposits in turbidite sequences: Their geology, geochemistry and history of the theories of their origin. Geological Association of Canada. Special paper 32:1-15.

Breislak, S., 1818. Institutions geologiques. Milan, 1:468.

Brooks, R.R., Chatterjee, A.K., Smith, P.K., Ryan, D.E. and H.F. Zhang, 1982. The distribution of gold in rocks and minerals of the Meguma Group of Nova Scotia, Canada. Nova Scotia Department of Mines and Energy. reprint 82-5.

Clarke, D.B. and A.N. Halliday, 1980. Strontium isotope geology of the South Mountain Batholith, Nova Scotia. Geochimica et Cosmochimica Acta,44:1045-1058.

Crocket, J.H., Fueton, F., Kabir, A. and P.M. Clifford, 1986. Distribution and localization of gold in Meguma Group Rocks, Nova Scotia: implications of metal distribution patterns in quartz veins and host rocks on mineralization processes at Harrigan Cove, Halifax County. Maritime Sediments and Atlantic Geology. 22:15- 33.

Dallymeyer, R.D. and J.D. Keppie, 1987. Polyphase late Paleozoic tectonothermal evolution of the southwestern Meguma Terrane, Nova Scotia: evidence from $^{40}Ar/^{39}Ar$ mineral ages. Canadian Journal of Earth Science. 24:1242-1254.

Eisbacher, G.H., 1969. Displacement and stress field along part of the Cobequid Fault, Nova Scotia. Canadian Journal of Earth Science, 6:1095-1104.

Faribault, E.R., 1899. The gold measures of Nova Scotia and deep mining. Journal Mining Society of Canada, 2:119-128.

Fyson, W.K., 1966. Structures in the Lower Paleozoic Meguma Group, Nova Scotia. Geological Society of America. bulletin 77:931-943.

Glasson, M.H. and R.R. Keays, 1978. Gold mobilization during cleavage development in sedimentary rocks from the auriferous slate belt of central Victoria, Australia; some important boundary conditions. Economic Geology. 73:496-511.

Graves, M.C., 1976a. The formation of gold bearing quartz veins in Nova Scotia: hydraulic fracturing under conditions of greenschist regional metamorphism during early stages of deformation. unpublished M.Sc. thesis, Dalhousie University, Halifax, Nova Scotia, p82-119.

----------, 1976b. Pre-folding Acadian emplacement of some gold-bearing quartz veins in southern Nova Scotia. Atlantic Geoscience Society Symposium Abstracts.

Graves, M.C. and M. Zentilli, 1982. A review of the geology of gold in Nova Scotia: in Geology of Canadian Gold Deposits. Hodder, R.W. and W. Petruk (eds.). The Canadian Institute of Mining and Metallurgy, special volume 24:233-242.

Henderson, J.R., 1983a. Harrigan Cove Mine. in CIM Geology Division Excursion Guidebook Gold Deposits in the Meguma Terrane of Nova Scotia, by Keppie, J.D., Haynes, S.J., Henderson, J.R., Smith, P.K., O'Brien, B.H., Zentilli, M., Jenson, L.R., MacEachren, I.J., Stea, R. and P . Rogers. Canadian Institute of Mining and Metallurgy. p104.

----------, 1983b. Analysis of structure as a factor controlling gold mineralization in Nova Scotia. Geological Society America, paper 83-1B. p13-21.

Henderson, M.N. and J.R. Henderson, 1986. Constraints on the origin of gold in the Meguma Zone, Ecum Secum area, Nova Scotia. Maritime Sediments and Atlantic Geology. 22:1-13.

Keppie, J.D., 1976. Structural modal for the saddle reef and associated gold veins in the Meguma Group, Nova Scotia. Nova Scotia Department of Mines, paper 76-1.

----------, 1982. The Minas Geofracture. Nova Scotia Department of Mines, reprint 82-4.

Keppie, J.D., Boyle, R.W. and S.J. Haynes, 1986. Turbidite-Hosted Gold Deposits. Geological Association of Canada special paper 32.

King, L.H. and B. MacLean, 1976. Geology of the Scotian shelf. Geological Survey of Canada. paper 74-31.

Kretschmar, U., 1983. Meguma-type turbidite hosted gold deposits in Nova Scotia. unpublished report prepared for the Geological Survey of Canada, p133.

Lemmlein, G.G., 1950. Al-bruni's mineralogical information. Moscow-Leningrad, Sbornik Biruni (collected papers) p106-127.

MacMichael, T.P., 1975. The origin of the lead-zinc-silver ores and the alteration of the surrounding granites at the Danbrack mine, Musquodoboit Harbour, Nova Scotia. B.Sc. thesis (Hons.), Dalhousie University, Halifax, Nova Scotia.

Malcolm, W., 1976. Gold fields of Nova Scotia. Geological Survey of Canada, memoir 385.

Mawer, C.K., 1986. The bedding-concordant gold-quartz veins of the Meguma Group, Nova Scotia: in Keppie, J.D., Boyle, R.W. and S.J. Haynes (eds.). Turbidite-Hosted Gold Deposits. Geological Association of Canada, special paper 32:135-148.

McBride, D.E., 1978. Geology of the Ecum Secum area, Halifax and Guysborough Counties, Nova Scotia. Nova Scotia Department of Mines, paper 78-1.

Muecke, G.K., Elias, P. and P.H. Reynolds, 1988. Hercynian/Alleghanian overprinting of an Acadian terrane: $^{40}Ar/^{39}Ar$ studies in the Meguma Zone, Nova Scotia, Canada. Chemical Geology. 73:153-167.

Newhouse, W.H., 1936. A zonal gold mineralization in Nova Scotia. Economic Geology, 31:805-831.

Poole, W.H., 1967. Tectonic evaluation of the Appalachian region of Canada: in Geology of the Atlantic Region. Neale, E.R.W. and H. Williams (eds.). Geological Association of Canada Special Paper 4:9-51.

----------, 1971. Graptolites, copper and potassium-argon in Goldenville Formation, Nova Scotia: in Report of Activities, part A. Geological Survey of Canada Special Paper 71-1A:9-11.

Poole, W.H., Sanford, B.V., Williams, H. and D.G. Kelly, 1970. Geology of Southeastern Canada: in Geology and Economic Minerals of Canada. Douglas, R.J.W. (ed.). Geological Survey of Canada, Economic Geology Report 1:229-304.

Ramsay, J.G., 1974. Development of chevron folds. Geological Society of America. bulletin 85:1741-1754.

Reynolds, P.H., Muecke, G.K. and E.E. Kublick, 1973. K-Ar dating of slates from the Meguma Group, Nova Scotia. Canadian Journal of Earth Science, 10:1059-1067.

Reynolds, P.H. and G.K. Muecke, 1978. Age studies on slates: applicability of the $^{40}Ar/^{39}Ar$ stepwise outgassing method. Earth and Planetary Science Letters, 40:111-118.

Reynolds, P.H., Zentilli, M. and G.K. Muecke, 1981. K-Ar and $^{40}Ar/^{39}Ar$ geochronology of granitoid rocks from southern Nova Scotia: its bearing on the geological evolution of the Meguma Zone of the Appalachians. Canadian Journal of Earth Science. 18:386-394.

Roedder, E., 1984. Fluid Inclusions. Mineralogical Society of America.

Schenk, P.E., 1970. Regional variation of the flysch-like Meguma Group of Nova Scotia compared to recent sedimentation off the Scotia shelf: in Lajoie, J. (ed.). Flysch Sedimentology in North America. Geological Association of Canada special paper 7:127-153.

----------, 1978. Synthesis of the Canadian Appalachians. Geological Survey of Canada, paper 78-13:111-136.

----------, 1981. The Meguma Zone of Nova Scotia - a remnant of Western Europe, South America or Africa?: in Kerr, J.W. and A,J, Ferguson (eds.). Geology of the North Atlantic Borderlands. memoir 7:119-148.

Seward, T.M., 1991. The hydrothermal geochemistry of gold: in Gold Metallogeny and Exploration. Foster, R.P. (ed.). Blackie, Toronto. p37-62.

Shenberger, D.M. and H.L. Barnes, 1989. Solubility of gold in aqueous sulphide solutions from 150° to 350°. Geochimica et Cosmochemica Acta, 53:269-278.

Sorby, H.C., 1858. On the microscope structure of crystals, indicating the origin of minerals and rocks. Geological Society of London Quarterly Journal. 14(1):453-500.

Spear, F.S. and J. Selverstone, 1983. Water exsolution from quartz: implications for the generation of retrograde metamorphic fluids. Geology. 11:82-85.

Stow, D.A.V., 1979. Distinguishing between fine-grained turbidites and contourites on the Nova Scotian deep-water margin. Sedimentology. 26:371-388.

Taylor, F.C. and E.A. Schiller, 1966. Metamorphism of the Meguma Group of Nova Scotia. Canadian Journal of Earth Science. 3:959-974.

Uematsu, M. and E.U. Franck, 1980. The static dielectric constant of water and steam. Journal of Physical Chemistry Reference Data, 9:1291-1301.

Waldron, J.W.F. and L.R. Jenson, 1985. Sedimentology of the Goldenville Formation, eastern shore, Nova Scotia. Geological Survey of Canada, paper 85-15.

Williams, H., 1978b. Geological development of the northern Appalachians: its bearing on the evolution of the British Isles: in Bowes, D.R. and B.E. Leake (eds.). Crustal Evolution in Northwestern Britain and Adjacent Regions. Seal House Press, Liverpool, England, p1-22.

Yoder, Jr., L.H. and B. MacLean, 1976. Geology of the Scotian shelf. Geological Survey of Canada, paper 74-31.